Double beta decay of some medium-mass nuclei

Master's thesis

Jaakko Maalampi

October 24, 2018

Instructor: Jouni Suhonen

Preface

I would like to thank my instructor for his patience in instructing my use of the BCS model.

Abstract:
This study examines the double beta decay of Zn-70, Se-80, Ru-104 and Cd-114. These nuclei are even, middle mass nuclei with open major shells. Their structure calls for the pairing interaction between like nucleons. In this study this is achieved by using the nuclear Bardeen-Cooper-Schrieffer (BCS) model. In the BCS model, the valence nucleons are treated as a sort of condensate that has spread across the valence energy levels. In the BCS model, interacting particles are replaced by non-interacting quasiparticles.

Double beta decay is a rare process, with only a handful of nuclei being predicted to experience them. The decay process involves accounting for the intermediate states between the initial and final nuclei. This is done by summing over the various possible levels, and weighing them by the occupation amplitudes of the level in question and dividing by the average energy between the initial and final states. An alternative proposal, the single-state-dominance hypothesis (SSDH), replaces this sum by assuming that only the ground state is relevant. This study uses the SSDH in its main results. The BCS double beta decay matrix elements were determined to be: Zn:0.91 Se:0.48 Ru:1.61 and Cd:0.95

The BCS results for the single beta decays of the intermediate nucleus are not wholly in agreement with the experimental $\log ft$ values. There are various possible error sources, the major one being that the basic BCS model assumes that the quasiparticles do not interact. There are extensions that allow correcting such things. As an alternative, I tested a model where the ground state of the intermediate nucleus was replaced by a linear combination of 1^+ states that could experience beta decay. The coefficients for these combinations were determined by requiring that one of the single beta decay $\log ft$ values is correct.

The aforementioned linear combinations were also used to calculate the double beta decay matrix element for each of the processes in this study. To evaluate these results, I also calculated the double beta decay matrix element using the single decay matrix elements that produced the experimental $\log ft$ values for the intermediate nucleus. This could have been achieved by calculating backwards from the $\log ft$ equation, but even more trivial was to take one linear combination that had been fitted to the corresponding process. These results were: Zn:0.045 Se:0.027 Ru:0.116 and Cd:0.076.

Tiivistelmä:
Tämä työ tarkastelee Zn-70, Se-80, Ru-104 ja Cd-114 ydinten kaksoisbeetahajoamista. Kyseiset ytimet ovat keskiraskaita parillisia ytimiä, joiden uloimmat kuoret ovat avoimia. Niiden rakenteeseen vaikuttaa voimakkaasti samanlaisten nukleonien välinen pariutumisvuorovaikutus. Tässä työssä tämä saavutetaan käyttämällä Bardeen-Cooper-Schrieffer (BCS) mallia ytimille. BCS mallissa uloimpia nukleoneja tarkastellaan eräänlaisena nesteenä, joka on levinnyt uloimpiin energiatasoihin. BCS mallissa keskenään vuorovaikuttavien hiukkasten sijasta tarkastellaan vuorovaikuttamattomia kvasihiukkasia.

Kaksoisbeetahajoaminen on harvinainen prosessi, vain muutamankymmenen ytimen ennustetaan pystyvän siihen. Hajoamisessa tulee ottaa huomioon alku- ja lopputilojen väliset tilat. Tämä huomioidaan summaamalla eri välitilojen kautta kulkevien prosessien matriisielementit yhteen ja painottamalla ne välitilojen energianimittäjillä. Vaihtoehtoisesti on olemassa nk. single state dominance hypothesis (SSDH), mikä sanoo että summan sijasta voidaan tarkastella vain väliytimen perustilaa. Tässä työssä käytetään SSDH:ta päätulosten laskemisessa. BCS kaksoisbeetamatriisielementit tarkasteltaville ytimille olivat: Zn:0.91 Se:0.48 Ru:1.61 ja Cd:0.95.

BCS mallin tuottamat arvot välitilojen beetahajoamisten log ft arvoille eivät vastaa kokeellisia arvoja tarkasti. On useita mahdollisia virhelähteitä, joista tärkein lienee se että kvasihiukkasten väliset vuorovaikutukset jätetään huomiotta perus BCS mallissa. BCS mallia voidaan laajentaa ottamaan nämä vuorovaikutukset huomioon. Laajentamisen sijaan testasin mallia missä väliytimen perustila korvataan 1^+ tilojen lineaarikombinaatiolla. Kombinaation kertoimet saadaan vaatimalla että kombinaatio tuottaa yhden kokeellisen log ft arvon.

Laskin kaksoisbeeta matriisielementit myös edellä mainittujen kombinaatioiden avulla. Arvioidakseni näitä tuloksia, laskin kaksoisbeetamatriisielementit myös käyttäen väliytimen kokeellisia tuloksia. Tämä olisi voitu saavuttaa laskemalla matriisielementti takaperin log ft arvosta, mutta samat matriisielementtien arvot tuotettiin lineaarikombinaatioiden sovituksessa, joten käytin niitä. Näin määritetyt kaksoisbeeta matriisielementit olivat: Zn:0.045 Se:0.027 Ru:0.116 ja Cd:0.076.

1 Introduction

This study examines the double beta decay of Zn-70, Se-80,Ru-104 and Cd-114. These nuclei are middle-mass with open major shells in the vicinity of the magic numbers. To determine the decay properties of these nuclei, a suitable model for their structures must be chosen. The simplest nuclear model involves examining a single particle in a mean field. Such models are suitable for nuclei at the magic numbers, as the large gap between major shells reduces the need to account for other interactions. Single particle mean field models are, however, unsuitable for this study, since nuclei in open major shells take far less energy to excite. The energy it takes to produce one particle-hole excitation is roughly equivalent to the energy taken to produce two particle or hole excitations [1, p. 370].

How should the model be improved? The single particle mean field interaction is the interaction between a particle and the other A-1 particles of a nucleus. The next level of interaction is the interaction between like particles, the pairing interaction. This interaction binds similar particles into J=0 pairs with isospin T=1. This leads to a variety of effects, such as even-even nuclei invariably having a ground state of 0^+. Additionally, the average mass between two neighboring even-even nuclei is lower than that of the even-odd nucleus between them [1, p.370-372]. The mass difference is known as the pairing gap and it is a crucial value in the following study.

What sort of a model is suitable for a nucleus that includes both the single particle mean field and the attractive pairing interaction between two particles? The situation is very similar to that of certain superconductors. There the electrons form cooper pairs due to the attractive interaction enabled by lattice vibrations. These electron pairs behave like bosons that have lower energy than individual electrons and can, in low temperatures, travel through the medium with no resistance. This description of superconductivity is part of the Bardeen-Cooper-Schrieffer or BCS theory of superconductivity [2]. This model can be applied to systems of many interacting particles that include a suitably strong pairing interaction. The nucleons for which the pairing interactions are strong are suitable for such an examination, see [3] and [4]. In this study, the nuclear BCS-model is used to describe the nucleus as a solid core surrounded by a layer of liquid pair condensate. The BCS-model is solvable numerically and this study uses a ready-made program to calculate the

BCS structure for each of the nuclei.

The main objective of this study is to determine the transition matrix element for the double beta decay for each of the nuclei. This involves determining the matrix elements for transitions to and from the in-between odd-odd nucleus. The processes being examined have experimental results for the beta decays of these odd-odd nuclei. Therefore, it will be possible to compare the theoretical predictions to the experimental results. In addition, I experimented with a method of fitting the experimental results into the calculation by assuming the intermediate state to be a superposition of proton-neutron quasiparticle states that fulfill the conditions necessary for beta decay.

2 BCS structure

The BCS theory was originally constructed to explain the properties of superconductors. It is based on noting that the exchange of phonons between electrons leads to an attractive interaction if the phonon energy is larger than the energy difference between the participating electron states[2]. The superconductor ground state, then, is a linear combination of these pairs with opposite spin and momentum. In the original study, Bardeen, Cooper and Schrieffer go on to derive the various properties of superconductors as being caused by this attractive interaction producing an energy gap below the critical temperature.

Applying the BCS model to the study of nuclear structure is not unexpected. There are a number of structural properties that are caused by nucleons experiencing a similar pairing interaction. Contrary to the superconductor case, the pairing interaction between nucleons is direct. This interaction, known as the pairing interaction, binds nucleons together into J=0 pairs. There are three types of pairs that could be formed: proton-proton, neutron-neutron and proton-neutron [5, chapter 1, section B2]. The last case is largely theoretical and only relevant for nuclei where the number of protons and neutrons is the same. This study concerns only nuclei with $N > Z$, so these mixed pairs needn't be accounted for. In this study, then, pairing is strictly between same types of particles.

As stated in the introduction, pairing leads to various phenomena in nuclei, but this study considers the analogue to the superconductor case, that is to say a

nucleus where the pairing interactions dominates the single-particle mean field model. In such a case, it is expected that the nucleon pairs would form some manner of condensate, similar to the superconductor ground state.

The BCS ground state of an even-even nucleus is [1, p. 392]

$$|BCS\rangle = \prod_a (u_a - v_a A_\alpha^\dagger)|CORE\rangle, \tag{1}$$

where u_a and v_a are the occupation amplitudes of the state a and $A_\alpha^\dagger$ creates a pair of like nucleons. The amplitudes are normalized so that $u_a^2 + v_a^2 = 1$. Structurally, the nuclear BCS model extends the nuclear mean field to account for pairing in the outermost nucleons. In (1), the core is the mean field vacuum of the hard center of the nucleus. The rest of the equation consists of adding back in the outermost nucleons in pairs. The ansatz shows that these levels have a distribution across the energy levels, determined by the occupation and inoccupation amplitudes v_a and u_a. Therefore the core of the nucleus can be said to be covered in a fermion liquid.

From the BCS ansatz it is then possible to derive the quasiparticle Hamiltonian etc. leading to the BCS equations [1, p. 401-402], which are as follows:

Occupation amplitudes

$$u_c = \theta^{(l_c)} \frac{1}{\sqrt{2}} \sqrt{1 + \frac{\eta_c}{E_c}}, \quad v_c = \frac{1}{\sqrt{2}} \sqrt{1 - \frac{\eta_c}{E_c}}. \tag{2}$$

Quasiparticle energy

$$E_c = \sqrt{\eta_c^2 + \Delta_c^2}. \tag{3}$$

Gap equation

$$2\widehat{j_b}\Delta_b = -\sum_a \frac{\widehat{j_a}\Delta_a}{E_a} \langle aa; 0|V|bb; 0\rangle. \tag{4}$$

Additionally, the average particle number is

$$\bar{n} = \sum_a \widehat{j_a^2} v_a^2. \tag{5}$$

In the above equations, $\theta^{(l_c)}$ is a phase factor, E_a is the quasiparticle energy of state a, and $\eta_c = \epsilon_c - \lambda - \mu_c$ is an energy term. In the previous, ϵ is the single particle energy, μ is a renormalization factor caused by interactions between nuclei and λ is the chemical potential, which is change in energy when a particle is added to the BCS ground state.

These equations can be solved iteratively, by choosing initial values for Δ and λ and using them to evaluate the various BCS equations. The condition for the completion of the calculation is that the average particle number is within a desired deviation from the exact particle number. The BCS vacuum forms a reference to be used to model the structure of the neighboring nuclei. The BCS calculations are done separately for protons and neutrons, since protons and neutrons don't generally pair together.

Particles in the BCS model are quasiparticles that have occupation amplitude. In even nuclei, the excitations have to overcome pairing, and therefore the lowest excitation energies are equivalent to the pairing gap energy. These excitations consist of an even number of quasiparticles, since both particles in the pair are excited. An odd nucleus has an unpaired particle, which is not paired. As a result, the excitation energy of a odd nucleus is far lower than the pairing gap energy. Additional excitations involve breaking a pair, leading to three- or more quasiparticle excitations.

2.1 Example

The example being considered throughout this study is the decay of Ruthenium-104 to Palladium-104. For that, both of the nuclei need to have their BCS structure numerically determined. This section examines Pd-104, but also includes the results for Ru-104.

First, the test case where $G_p = G_n = 1$ is used to determine the state with the lowest quasiparticle energy. Since palladium-104 is even-even, any single particle excitation has to break a pair. Thus, all of the quasiparticle energies have to be equal or greater than the pairing gap energy. The pairing gap for both protons and neutrons can be calculated using measured separation energies [1, p 500]:

$$
\begin{aligned}
\Delta_p(A,Z) &= \frac{1}{4}(-1)^{Z+1}(S_p(A+1,Z+1) - 2\cdot S_p(A,Z) + S_p(A-1,Z-1)) \\
&= \frac{-1}{4}\cdot(4965\,\mathrm{keV} - 2\cdot 8655.9\,\mathrm{keV} + 6214.1\,\mathrm{keV}) = 1533.175\,\mathrm{keV} \\
\Delta_n(A,Z) &= \frac{1}{4}(-1)^{A-Z+1}(S_n(A+1,Z) - 2\cdot S_n(A,Z) + S_n(A-1,Z)) \\
&= \frac{-1}{4}\cdot(7094.1\,\mathrm{keV} - 2\cdot 9981.3\,\mathrm{keV} + 7625.4\,\mathrm{keV}) = 1310.775\,\mathrm{keV}.
\end{aligned}
\tag{6}
$$

Separation energies are tabulated for example in [6]. At this point the pairing strength parameters are altered until the lowest quasiparticle states fulfill the requirements $E_{qp}(lowest) = \Delta$. These conditions are fulfilled in Pd-114 by pairing strengths $G_n = 0.98575$ and $G_p = 1.11806$. For Ru-104, the parameters are $G_n = 1.02167$ and $G_p = 1.11278$. Tables 1- 4 contain the BCS results needed for the example case.

Table 1: BCS results for neutrons in Ru-104. The included values are: the quantum numbers of the single particle energy levels of Ru-104, the occupation and unoccupation amplitudes and the quasiparticle energies.

nlj	u	v	E_{qp}
$1p_{\frac{1}{2}}$	0.10755	0.99420	7.87388
$1p_{\frac{3}{2}}$	0.09345	0.99562	9.25947
$0f_{\frac{5}{2}}$	0.08051	0.99675	9.52388
$0f_{\frac{7}{2}}$	0.06875	0.99763	13.16101
$2s_{\frac{1}{2}}$	0.85958	0.51101	1.47076
$1d_{\frac{3}{2}}$	0.92607	0.37736	1.95223
$1d_{\frac{5}{2}}$	0.44304	0.89650	1.75067
$0g_{\frac{7}{2}}$	0.73205	0.68125	1.41516
$0g_{\frac{9}{2}}$	0.14793	0.98900	5.65585
$0h_{\frac{9}{2}}$	0.99820	0.05999	10.00966
$0h_{\frac{11}{2}}$	0.97080	0.23991	2.92117

Table 2: BCS results for protons in Ru-104. Same structure as above.

nlj	u	v	E_{qp}
$1p_{\frac{1}{2}}$	0.49107	0.87112	2.19579
$1p_{\frac{3}{2}}$	0.29007	0.95701	3.37754
$0f_{\frac{5}{2}}$	0.28854	0.95747	3.93466
$0f_{\frac{7}{2}}$	0.11820	0.99299	7.86274
$2s_{\frac{1}{2}}$	0.99867	0.05161	7.75299
$1d_{\frac{3}{2}}$	0.99763	0.06885	8.58665
$1d_{\frac{5}{2}}$	0.99496	0.10023	5.57999
$0g_{\frac{7}{2}}$	0.98971	0.14309	6.85861
$0g_{\frac{9}{2}}$	0.69994	0.71420	1.54905
$0h_{\frac{9}{2}}$	0.99900	0.04461	17.06545
$0h_{\frac{11}{2}}$	0.99745	0.07135	8.11898

Table 3: Palladium-104 BCS results for neutrons

nlj	u	v	E_{qp}
$1p_{\frac{1}{2}}$	0.10201	0.99478	7.58583
$1p_{\frac{3}{2}}$	0.08536	0.99635	8.99623
$0f_{\frac{5}{2}}$	0.07281	0.99735	9.27618
$0f_{\frac{7}{2}}$	0.06177	0.99809	12.97503
$2s_{\frac{1}{2}}$	0.92733	0.37424	1.59549
$1d_{\frac{3}{2}}$	0.95455	0.29804	2.22782
$1d_{\frac{5}{2}}$	0.49901	0.86659	1.41554
$0g_{\frac{7}{2}}$	0.81626	0.57768	1.31078
$0g_{\frac{9}{2}}$	0.13772	0.99047	5.38812
$0h_{\frac{9}{2}}$	0.99875	0.05001	10.50228
$0h_{\frac{11}{2}}$	0.98040	0.19704	3.13048

Table 4: Palladium-104 BCS results for protons

nlj	u	v	E_{qp}
$1p_{\frac{1}{2}}$	0.40415	0.91469	2.35481
$1p_{\frac{3}{2}}$	0.24125	0.97046	3.69255
$0f_{\frac{5}{2}}$	0.24755	0.96887	4.24532
$0f_{\frac{7}{2}}$	0.10493	0.99448	8.22503
$2s_{\frac{1}{2}}$	0.99853	0.05411	7.06337
$1d_{\frac{3}{2}}$	0.99745	0.07138	7.81791
$1d_{\frac{5}{2}}$	0.99432	0.10644	4.91745
$0g_{\frac{7}{2}}$	0.98917	0.14676	6.28039
$0g_{\frac{9}{2}}$	0.57730	0.81653	1.53318
$0h_{\frac{9}{2}}$	0.99903	0.04395	16.30645
$0h_{\frac{11}{2}}$	0.99741	0.07194	7.54543

The pairing interaction causes the changes in the nuclear structure, figures 1 and 2 show the occupation amplitude for each of the single particle energy levels of Pd-104. The figures also show how the structure of the nucleus changes as the pairing strength parameter is increased or reduced. The figures show that the nucleons have spread outside of the Fermi surface. The magnitude of this effect is clearly related to the size of the pairing strength parameter.

Since the BCS results form a reference, the structure of neighboring nuclei can be probed by using the quasiparticle energy levels. Figures 3 and 4 show the normalized quasiparticle energy levels and the corresponding experimental energy levels of the nucleus with one additional nucleon of the corresponding type. The normalization has removed the pairing gap energy, so the lowest quasiparticle excitation should be equivalent to a single particle excitation.

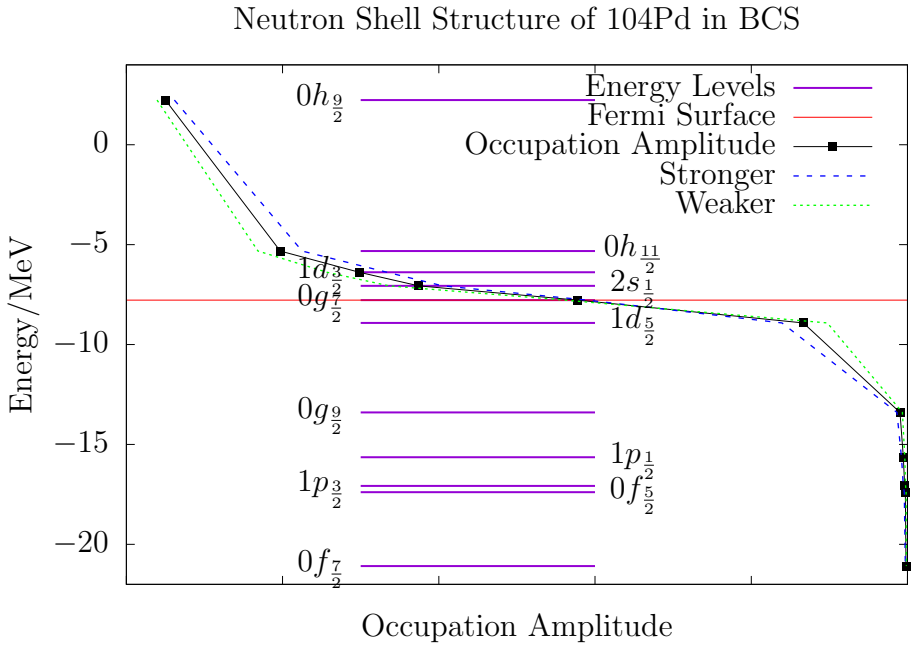

Figure 1: The occupation amplitude for neutron single particle states of Pd-104. The x-axis is the occupation amplitude and runs from 0 to 1. This tends to lower as the energy of the states increases. Stronger pairing leads to further deformation about the Fermi surface.

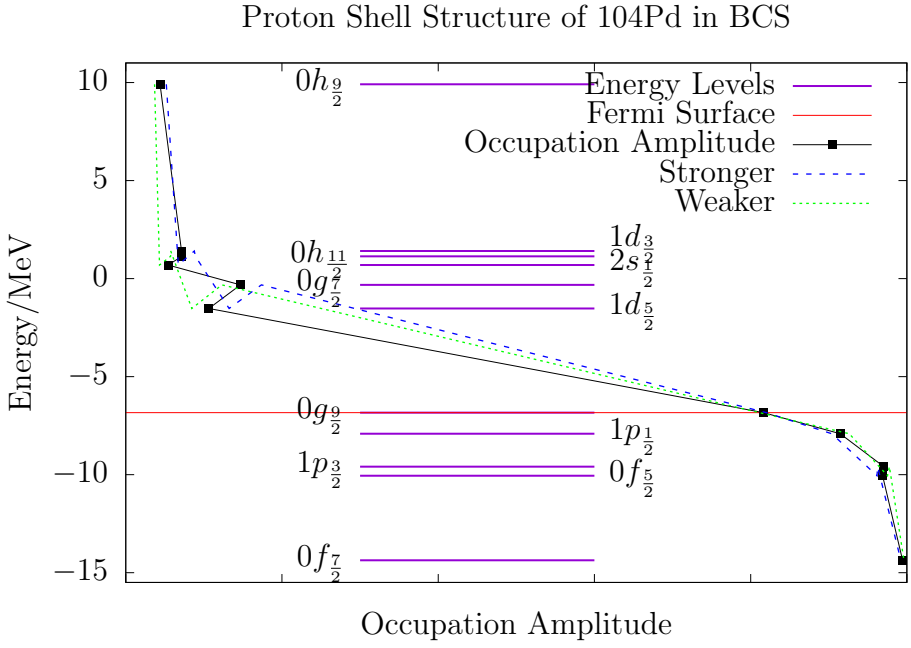

Figure 2: The occupation amplitude in the proton case. The x-axis is the occupation amplitude and runs from 0 to 1. In this case, there are points of increased occupation amplitude at $1p_{\frac{3}{2}}$, $0g_{\frac{7}{2}}$, $0h_{\frac{11}{2}}$ and $1d_{\frac{3}{2}}$.

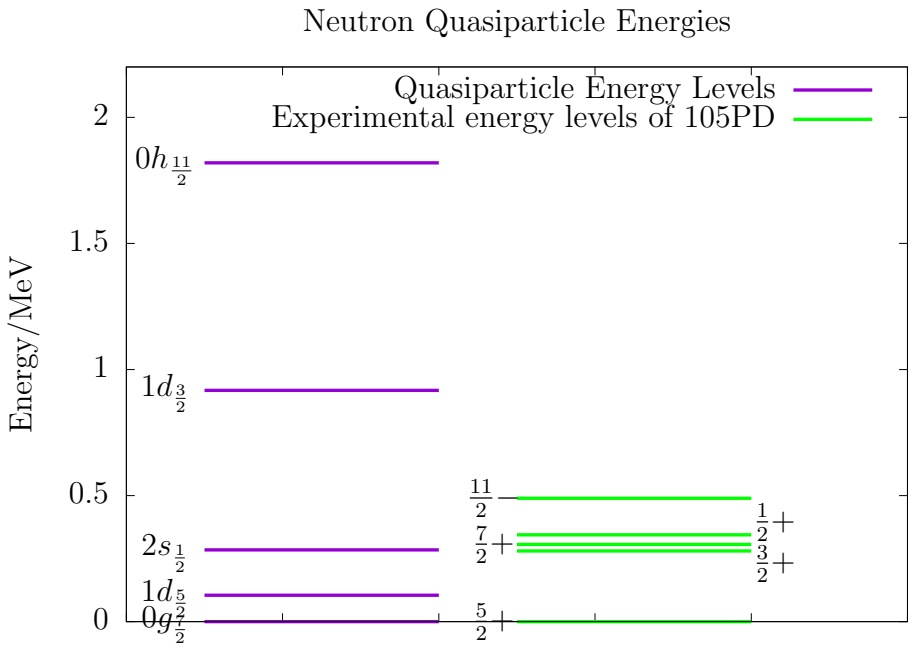

Figure 3: The normalized neutron quasiparticle energy levels and the lowest energy levels of palladium-105. Pd-105 has a single non-paired neutron, so its neutron excitations do not require breaking a pair, so the excitations are lower than the pairing gap [7, page 135]. The quasiparticle d levels are both higher than the corresponding levels of the experimental spectrum. The rest of the states are correctly ordered and their relative positions resemble the experimental spectrum.

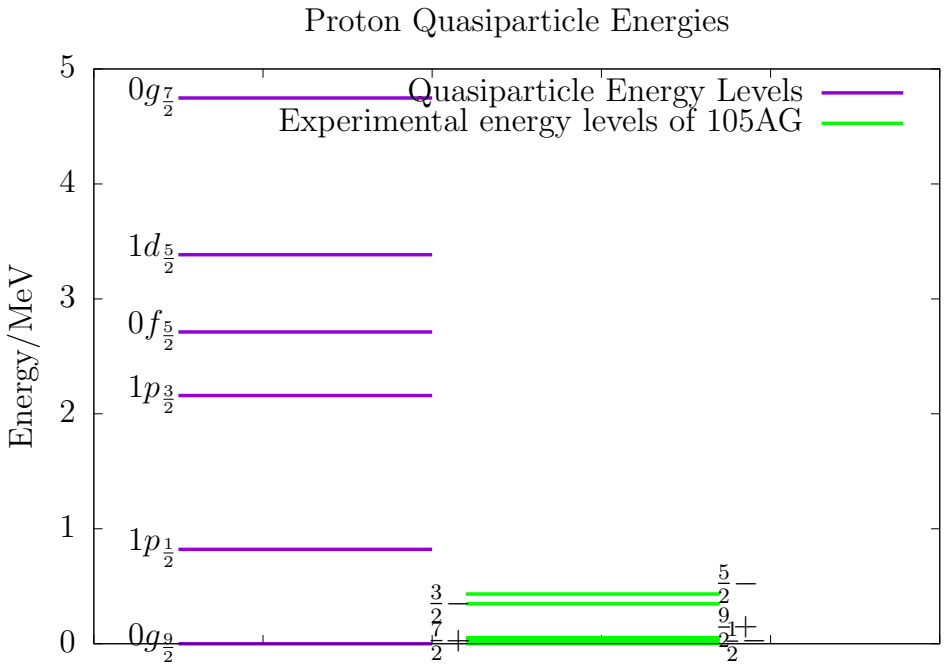

Figure 4: The normalized energy levels of proton quasiparticles compared to silver-105. The occupation amplitude spike at $0g_{\frac{7}{2}}$ leads to a high quasiparticle energy. The positions of $0g_{\frac{9}{2}}$ and $1p_{\frac{1}{2}}$ are also inverted.

3 Decay calculations

3.1 Beta decay in BCS formalism

The half-life of a decay process is related to the transition probability by

$$t_{\frac{1}{2}} = \frac{\ln 2}{T_{fi}}. \tag{7}$$

The transition probability T_{fi} can be calculated by using Fermi's golden rule. What follows is the transition probability for beta decay with the addition of the BCS formalism. The reduced single-particle matrix element for Gamow-Teller transitions is: [1, p. 165]

$$M_{GT}(ab) = \sqrt{2}\delta_{n_a n_b}\delta_{l_a l_b}\hat{j}_a\hat{j}_b(-1)^{l_a+j_a+\frac{3}{2}} \begin{Bmatrix} \frac{1}{2} & \frac{1}{2} & 1 \\ j_b & j_a & l_a \end{Bmatrix}, \tag{8}$$

where the last term is the Wigner-6j symbol, which is related to the coupling of three angular momenta and is calculated in some detail in appendix A. Equations (9) and (10) are the Gamow-Teller matrix elements for a transition from a two-quasiparticle state with angular momentum J to the BCS vacuum. For later use, (11) is the relation between transitions from and to the two-quasiparticle state [1, p. 461].

$$M_{GT}^{(+)}(pnJ \to BCS) = -\delta_{J1}\sqrt{3}v_n u_p M_{GT}(pn). \tag{9}$$

$$M_{GT}^{(-)}(pnJ \to BCS) = \delta_{J1}\sqrt{3}v_p u_n M_{GT}(pn) \tag{10}$$

$$M_{GT}^{(\mp)}(BCS \to pnJ) = (-1)^J M_J^{\pm}(pnJ \to BCS) \tag{11}$$

Additionally, it is possible to deal with linear combinations of two-quasiparticle states. In such cases

$$M_{GT}^{(\pm)}(pnJ \to BCS) = \sum_i \alpha_i \delta_{J1}\sqrt{3}u_i v_i M_{GT}(pn), \tag{12}$$

where u_i and v_i are the amplitudes of the corresponding quasiparticle states.

The Gamow-Teller reduced transition probability is [1, p. 163]

$$B_{GT} = \frac{g_a^2}{2J_i + 1} \left| M_{GT}^{(\pm)} \right|^2, \tag{13}$$

where $g_a = 1.27$ is a constant. The transition probability for beta decay is

$$T_{fi} = \frac{\kappa / \ln 2}{f(B_F + B_{GT})}, \tag{14}$$

where $\kappa = \frac{2\pi^3 \hbar^7 \ln 2}{m_e^5 c^4 G_F^2} = 6147s$, f is the structural integral and B_F is the reduced transition probability for Fermi-type transitions. Such transitions are suppressed in the beta decay case, so the $\log ft$ value for a beta decay is

$$\log f_0 t_{\frac{1}{2}} = \log \frac{\kappa}{B_{GT}} \tag{15}$$

3.1.1 Example

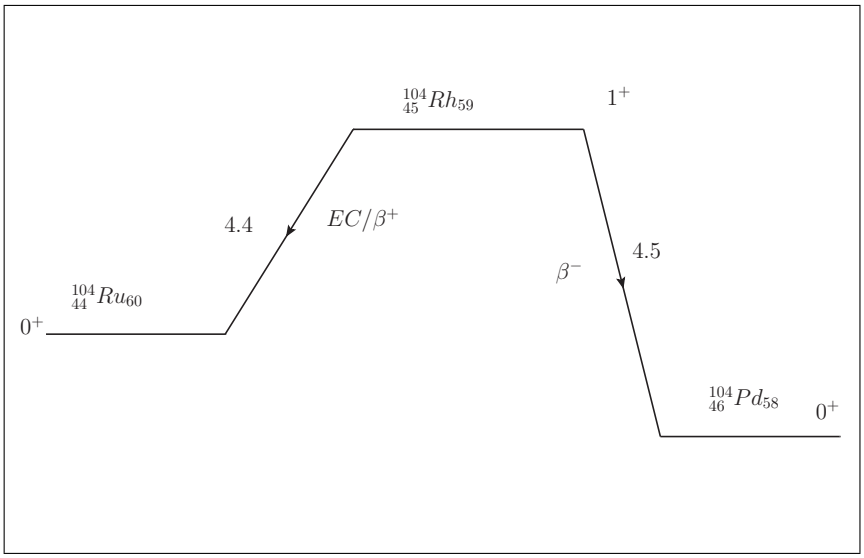

Figure 5: The decay modes of Rhodium-104. The values are the experimental $\log ft$ values of the corresponding decay.

Consider a transition from the Rh-104 ground state to the Ru-104 BCS vacuum, as seen in 5. Now the matrix element is

$$\begin{aligned} M_{GT}(1g_{\frac{9}{2}}, 1g_{\frac{7}{2}}) &= \sqrt{2}\delta_{1,1}\delta_{4,4}\sqrt{9+1}\sqrt{7+1}(-1)^{4+\frac{9}{2}+\frac{3}{2}} \begin{Bmatrix} \frac{1}{2} & \frac{1}{2} & 1 \\ \frac{9}{2} & \frac{7}{2} & 4 \end{Bmatrix} \\ &= \sqrt{160}(-\frac{\sqrt{3}}{9}) \\ &= -\frac{4\sqrt{30}}{9}, \end{aligned} \tag{16}$$

and with the addition of BCS results from tables 1 and 2,

$$\begin{aligned} M_{GT}^{(+)}(1g_{\frac{9}{2}}, 1g_{\frac{7}{2}} 1^+ \to 0^+) &= -\delta_{1,1}\sqrt{3} \cdot 0.68125 \cdot 0.69994 \cdot (-\frac{4\sqrt{30}}{9}) \\ &\approx 1.42165\sqrt{2} \approx 2.0105 \end{aligned} \tag{17}$$

For later use, the same mother nucleus decaying into the palladium-104 vacuum has the matrix element

$$M_{GT}^{(-)}(1g_{\frac{9}{2}}, 1g_{\frac{7}{2}} 1^+ \to 0^+) = \delta_{11}\sqrt{3} \cdot 0.81653 \cdot 0.81626 \cdot (-\frac{4\sqrt{30}}{9}) \approx 2.8102. \tag{18}$$

The reduced transition probability for the example decay is

$$B_{GT} = \frac{1.27^2}{2+1}(1.42165\sqrt{2})^2 \approx 2.1732. \tag{19}$$

Finally, the $\log ft$ value for this decay is

$$\log f_0 t_{\frac{1}{2}} = \log \frac{6147}{2.17320} \approx 3.452 \approx 3.45. \tag{20}$$

The experimental value is 4.4, per [8].

3.2 Linear approximation of the initial state

Suppose that the initial state is approximated by a linear combination of two states,

$$|\Psi_i\rangle = \alpha_1|\Psi_1\rangle + \alpha_2|\Psi_2\rangle. \tag{21}$$

Further, suppose that both α are real and normalized, i.e.

$$\alpha_1^2 + \alpha_2^2 = 1. \tag{22}$$

Suppose that such a state experiences β^+ decay. Then (12) reads

$$M_{GT}^{(+)}(J_i^+ \to J_f^+) = -\sqrt{3}(\alpha_1 v_{\nu_1} u_{\pi_1} M_{GT}(\pi_1, \nu_1) + \alpha_2 v_{\nu_2} u_{\pi_2} M_{GT}(\pi_2, \nu_2)). \tag{23}$$

Note that the differences between equations (9) and (10) are the overall sign and which states u and v amplitudes are used. Simplify the notation by writing

$$A_i = v_i u_i M(\pi_i, \nu_i), \tag{24}$$

where v_i and u_i are either v_π and u_ν or vice-versa, depending on the decay process. This will help in generalizing the results to cover both types of decay. Rearranging (15) produces the following

$$\log ft = \log \frac{\kappa}{B_{GT}} = \log \frac{3\kappa}{g_a^2} - 2 \log \left| M_{GT}^{(+)}(1^+ \to 0^+) \right|, \tag{25}$$

and further

$$\left| M_{GT}(J_i^+ \to J_f^+) \right| = \sqrt{\frac{3\kappa}{g_a^2 ft}}. \tag{26}$$

Inserting equation (23) into the above and using the simplified notation from equation (24) gives

$$\left| -\sqrt{3}(\alpha_1 A_1 + \alpha_2 A_2) \right| = \sqrt{\frac{3\kappa}{g_a^2 ft}}, \tag{27}$$

which can be further simplified to

$$|(\alpha_1 A_1 + \alpha_2 A_2)| = \sqrt{\frac{\kappa}{g_a^2 ft}}. \tag{28}$$

The calculations up to this point have assumed that the beta decay is β^+. With the choice of notation, the differences between β^+ and β^- decays have been absorbed, and the following calculations are the same for both processes. Notation is further simplified by

$$C(ft) = \sqrt{\frac{\kappa}{g_a^2 ft}}. \tag{29}$$

Opening the norm produces two cases,

$$\alpha_1 A_1 + \alpha_2 A_2 = \pm C(ft). \tag{30}$$

Solving α_1 from the above is simple:

$$\alpha_1 = \frac{\pm C(ft) - \alpha_2 A_2}{A_1}. \tag{31}$$

Insert the above into the normalization condition (22)

$$(\frac{\pm C(ft) - \alpha_2 A_2}{A_1})^2 + \alpha_2^2 = 1. \tag{32}$$

$$(\pm C(ft) - \alpha_2 A_2)^2 + \alpha_2^2 A_1^2 = A_1^2 \tag{33}$$

$$\alpha_2^2(A_1^2 + A_2^2) \mp \alpha_2(2A_2 C(ft)) + C^2(ft) - A_1^2 = 0 \tag{34}$$

This is a second order polynomial and thus

$$\alpha_2 = \frac{\pm 2A_2 C(ft) \pm \sqrt{(2A_2 C(ft))^2 - 4(A_1^2 + A_2^2)(C^2(ft) - A_1^2)}}{2(A_1^2 + A_2^2)}. \tag{35}$$

Note that the first $\pm$ comes from norm in equation (28) and is therefore independent of the other. There are up to four possible values for α_2. Two of the possible values can be ruled out by assuming that α_1 is positive. This can be done because if (26) is fulfilled by some (α_1, α_2) pair, it is also fulfilled by $(-\alpha_1, -\alpha_2)$. Therefore it is sensible to only examine those combinations where the ground state has a positive coefficient.

3.2.1 Requirements for the realness of α_2

α_2 is real if and only if

$$\begin{aligned}
(2A_2 C(ft))^2 - 4(A_1^2 + A_2^2)(C^2(ft) - A_1^2) &\geq 0 \\
4(A_1^2 + A_2^2)A_1^2 &\geq 4(A_1^2 + A_2^2)C^2 - (2A_2 C)^2 = 4A_1^2 C^2 \\
A_1^2 + A_2^2 &\geq C^2 \\
[u_1 v_1 M(p_1, n_1)]^2 + [u_2 v_2 M(p_2, n_2)]^2 &\geq \frac{\kappa}{g_a^2 ft} \approx \frac{3811}{ft}.
\end{aligned} \tag{36}$$

Therefore this approximation method is not valid for all decay processes. The right side decreases as the ft value of the decay increases, so this method is more likely to be valid for slow processes, with a $\log ft$ value of more than 3 being the minimum requirement.

3.2.2 Choosing states

This method assumes that the participating states can contribute to the decay process, i.e.

$$\begin{aligned} \delta_{n_\pi n_\nu} &= 1 \\ \delta_{l_\pi l_\nu} &= 1. \end{aligned} \tag{37}$$

Further, the angular momenta of the proton and neutron states should conform to

$$j_\pi + j_\nu \geq j_i \geq |j_\pi - j_\nu| \,, \tag{38}$$

where j_i is the angular momentum of the nucleus that decays, in this case $j_i = 1$. Choosing from amongst the proton-neutron combined states that fulfill these conditions is done by minimizing the sum of the quasiparticle-energies of the participant states. This condition means that we have chosen the lowest state of given spin-parity in the decaying odd-odd nucleus.

3.2.3 Calculations

Continuing from the previous example, the first state at the Fermi surface is $p = 0g_{\frac{9}{2}}, n = 0g_{\frac{7}{2}}$ and the second is $p = 0g_{\frac{9}{2}}$, $n = 0g_{\frac{9}{2}}$. As seen in the tables 1 and 2, the corresponding occupation amplitudes are:

$$\begin{aligned} u_p &= 0.69994 \\ v_n &= 0.989 \end{aligned} \tag{39}$$

Thus (24) is of the form

$$\begin{aligned} A_1 &= v_{n1}u_{p1}M_{GT}(0g_{\frac{9}{2}}, 0g_{\frac{7}{2}}) = 0.68125 \cdot 0.69994 \cdot (-0.9938\sqrt{6}) \\ &\approx -0.47388\sqrt{6} \approx -1.1608 \\ A_2 &= v_{n2}u_{p2}M_{GT}(0g_{\frac{9}{2}}, 0g_{\frac{9}{2}}) = 0.989 \cdot 0.69994 \cdot (0.1111\sqrt{330}) \\ &\approx 0.07691\sqrt{330} \approx 1.3972. \end{aligned} \tag{40}$$

The experimental logft value for this decay is 4.4. Then (29) is

$$C(4.4) = \sqrt{\frac{6147}{1.27^2 \cdot 10^{4.4}}} \approx 0.38952 \tag{41}$$

Substituting these values into (35) leads to

$$\begin{aligned} \alpha_2 &= \frac{\pm 2 \cdot 1.4 \cdot 0.39}{2((-1.161)^2 + 1.40^2)} \\ &\pm \frac{\sqrt{(2 \cdot 1.40 \cdot 0.39)^2 - 4((-1.161)^2 + 1.40^2)(0.39^2 - (-1.161)^2)}}{2((-1.161)^2 + 1.40^2)} \\ &= \pm(-0.1651) \pm 0.6235 \\ &= \begin{cases} 0.7891 & ++ \\ -0.4592 & +- \\ 0.4592 & -+ \\ -0.7891 & -- \end{cases} \end{aligned} \tag{42}$$

Equation (31) can then be used to determine the values of α_1:

$$\alpha_1 = \frac{\pm C(ft) - \alpha_2 A_2}{A_1} = \frac{0.38952 - 0.7891 \cdot 1.3972}{-1.1608} = 0.6143. \tag{43}$$

Similarly for the other distinct value, $\alpha_1 = -0.8883$. The rest of the values are simply negations of the ones already calculated. By requiring α_1 to be positive, the number of possible values are reduced by two. Finally, the coefficients that produce the experimental results for this decay are:

$$(\alpha_1, \alpha_2) = \begin{cases} (0.6143, 0.7891) \\ (0.8883, 0.4592) \end{cases} \tag{44}$$

These values can be used in (12) to calculate the logft value for a decay from this linear combination to the BCS vacuum. Using (40) and the first pair of alphas, the matrix element (9) is now

$$\begin{aligned} M_{GT}^{(+)}(1^+ \to 0^+) &= \alpha_1\sqrt{3}u_1v_1M_{GT}(pn)_1 + \alpha_2\sqrt{3}u_2v_2M_{GT}(pn)_2 \\ &= 0.6143\sqrt{3}\cdot(-1.1608) + 0.7891\sqrt{3}\cdot 1.3972 \\ &\approx -0.67455. \end{aligned} \tag{45}$$

From here the calculations proceed as before. $B_{GT} \approx 0.24463$ and $\log ft = 4.40015 \approx 4.4$. The same values are also produced by the other pair of coefficients. The key difference between the different combinations is their behavior when calculating the other beta decay mode, since there are no conditions imposed upon it. Now,

$$\begin{aligned} (\alpha_1, \alpha_2) = (0.6143, 0.7891) &\overset{\beta^-}{\Rightarrow} \log ft = 3.76 \\ (\alpha_1, \alpha_2) = (0.8883, 0.4592) &\Rightarrow \log ft = 3.329 \approx 3.33. \end{aligned} \tag{46}$$

As the experimental value for the $\log ft$ of this process is 4.5, it is clear that the model in use does not reproduce for this decay mode.

Similarly, fitting the linear combination to the β^- decay from Rh-104 to Pd-104 leads to the following sets of coefficients

$$\begin{aligned} (\alpha_1, \alpha_2) = (0.345, 0.939) &\overset{\beta^+}{\Rightarrow} \log ft = 3.66 \\ (\alpha_1, \alpha_2) = (0.074, -0.997) &\Rightarrow \log ft = 3.24 \end{aligned} \tag{47}$$

3.2.4 Three-state linear approximation

The three-state approximation follows from the previous calculations with some adaptation of notation. Let (α_1, α_2) be the linear coefficients calculated by the previous method. Assume now that the initial state can now be approximated by

$$|\Psi_i\rangle = \beta_1(\alpha_1|\Psi_1\rangle + \alpha_2|\Psi_2\rangle) + \beta_2|\Psi_3\rangle). \tag{48}$$

If $\beta_1^2 + \beta_2^2 = 1$, then

$$\begin{aligned}\langle\Psi_i|\Psi_i\rangle &= \beta_1^2\alpha_1^2 + \beta_1^2\alpha_2^2 + \beta_2^2 \\ &= \beta_1^2(\alpha_1^2 + \alpha_2^2) + \beta_2^2 \\ &= \beta_1^2 + \beta_2^2 = 1.\end{aligned} \tag{49}$$

The β-coefficients can be calculated in exactly the same way as the α-coefficients, with the following substitutions

$$\begin{aligned}\alpha_i &= \beta_i \\ A_1 &= \alpha_1 v_1 u_1 M(\pi_1, \nu_1) + \alpha_2 v_2 u_2 M(\pi_2, \nu_2) \\ A_2 &= v_3 u_3 M(\pi_3, \nu_3).\end{aligned} \tag{50}$$

3.2.5 Calculations

Continue the approximation by choosing to use $(\alpha_1, \alpha_2) = (0.6143, 0.7891)$. Using the palladium-104 BCS vacuum, the three states used in the approximation are:

$$\begin{aligned}|\Psi_1\rangle &= |p : 0g_{\frac{9}{2}}\ v_p = 0.81653, n : 0g_{\frac{7}{2}}\ u_n = 0.81626\rangle \\ |\Psi_2\rangle &= |p : 0g_{\frac{9}{2}}\ v_p = 0.81653, n : 0g_{\frac{9}{2}}\ u_n = 0.13772\rangle \\ |\Psi_3\rangle &= |p : 1d_{\frac{5}{2}}\ v_p = 0.10644, n : 1d_{\frac{5}{2}}\ u_n = 0.49901\rangle\end{aligned} \tag{51}$$

Now, using the substitutions in (50) and calculating the M terms:

$$\begin{aligned}A_1 &= 0.6143 \cdot 0.81653 \cdot 0.81626 \cdot (-0.99381\sqrt{6}) \\ &\quad + 0.7891 \cdot 0.81653 \cdot 0.13772 \cdot (0.1111\sqrt{330}) \\ &= 0.0099\sqrt{30} - 0.4069\sqrt{6} \\ &\approx -0.8176 \\ A_2 &= 0.10644 \cdot 0.49901 \cdot 0.2\sqrt{70} = 0.01062\sqrt{70} \approx 0.0889.\end{aligned} \tag{52}$$

The expected logft value of Rh-104 decaying into Pd-104 is 4.5, therefore

$$C(4.5) = 0.34716. \tag{53}$$

Inserting these values into (35) and substituting $\beta_i = \alpha_i$ gives

$$(\beta_1, \beta_2) = \begin{cases} (-0.3217, 0.9468) & ++ \\ (-0.5176, -0.8556) & +- \\ (0.5176, 0.8556) & -+ \\ (0.3217, -0.9468) & -- . \end{cases} \tag{54}$$

To maintain the sign of the first coefficient, assume that $\beta_1 > 0$, then

$$(\alpha_1, \alpha_2, \alpha_3) = \begin{cases} (0.318, 0.408, 0.856) \\ (0.198, 0.254, -0.947). \end{cases} \tag{55}$$

Using these values to calculate the $\log ft$ decay value again leads to the experimental value of 4.5. How do these combinations behave in the other decay mode?

$$\begin{aligned} (\alpha_1, \alpha_2, \alpha_3) = (0.318, 0.408, 0.856) &\overset{\beta^+}{\Rightarrow} \log ft \approx 3.24 \\ (\alpha_1, \alpha_2, \alpha_3) = (0.1919, -0.1793, -0.9649) &\Rightarrow \log ft \approx 3.61 \end{aligned} \tag{56}$$

For the latter set of alphas:

$$\begin{aligned} (\alpha_1, \alpha_2, \alpha_3) = (0.287, 0.148, 0.947) &\overset{\beta^+}{\Rightarrow} \log ft \approx 3.36 \\ (\alpha_1, \alpha_2, \alpha_3) = (0.173, 0.089, -0.981) &\Rightarrow \log ft \approx 3.21 \end{aligned} \tag{57}$$

Alternatively, using the first alphas from (47),

$$\begin{aligned} (\alpha_1, \alpha_2, \alpha_3) = (0.327, 0.890, -0.318) &\overset{\beta^-}{\Rightarrow} \log ft \approx 4.48 \\ (\alpha_1, \alpha_2, \alpha_3) = (0.247, 0.672, -0.698) &\Rightarrow \log ft \approx 4.60, \end{aligned} \tag{58}$$

and for the latter pair:

$$\begin{aligned} (\alpha_1, \alpha_2, \alpha_3) = (0.042, -0.566, 0.823) &\overset{\beta^-}{\Rightarrow} \log ft \approx 4.55 \\ (\alpha_1, \alpha_2, \alpha_3) = (0.062, -0.826, 0.560) &\Rightarrow \log ft \approx 4.83. \end{aligned} \tag{59}$$

3.3 Double Beta decay

The double beta decay matrix element is more complex than the one of the single decay, since the process has two steps. The Gamow-Teller matrix element for the double beta decay is of the form [9, eqn 7.31]

$$M_{GT}^{2\nu} = \sum_j \frac{\langle 0_f^+ | t_- \sigma | 1_j^+ \rangle \langle 1_j^+ | t_- \sigma | 0_i^+ \rangle}{E_j - E_i + Q_{\beta\beta}/2 + m_e}. \tag{60}$$

The numerator in (60) is just the matrix elements for the two beta decays from the initial state to the intermediate state and from the intermediate state to the final state. The denominator is the energy difference between the intermediate state j and the average energy of the initial and final states. Thus, the choice of the intermediate state j is weighted by this difference in energy, which is shown in 6. In this study, we will exclude the sum over the intermediate states by using the single-state-dominance hypothesis, wherein it is assumed that the ground state is dominant [10]. The double beta decay matrix element can now be written as follows, with some alterations to the denominator due to different formalism:

$$\begin{aligned} \left| M_{DGT}^{(2\nu)}(0^+ \to 0^+) \right| &= \left| \frac{M_{GT}^{(-)}(BCS \to pnJ) M_{GT}^{(-)}(pnJ \to BCS)}{(\frac{1}{2}Q_{\beta\beta} + \Delta)/m_e c^2 + 1} \right| \\ &= \left| \frac{M_{GT}^{(+)}(pnJ \to BCS) M_{GT}^{(-)}(pnJ \to BCS)}{(\frac{1}{2}Q_{\beta\beta} + \Delta)/m_e c^2 + 1} \right| \end{aligned} \tag{61}$$

where $Q_{\beta\beta}$ is the Q value of the process, and $\Delta = Q_{ec} - m_e c^2$ is the Q value of the electron capture process, excluding the energy of the electron. The $Q_{\beta\beta}$ and Q_{EC} values are related, as

$$Q_{\beta\beta} = Q_{\beta^-} - Q_{EC}. \tag{62}$$

The Q values can be found, for example, in [11]. In (61), the transition matrix from the initial state is converted to the positive beta decay matrix element using (11). Figure 6 shows the value of the denominator is determined for each intermediate state.

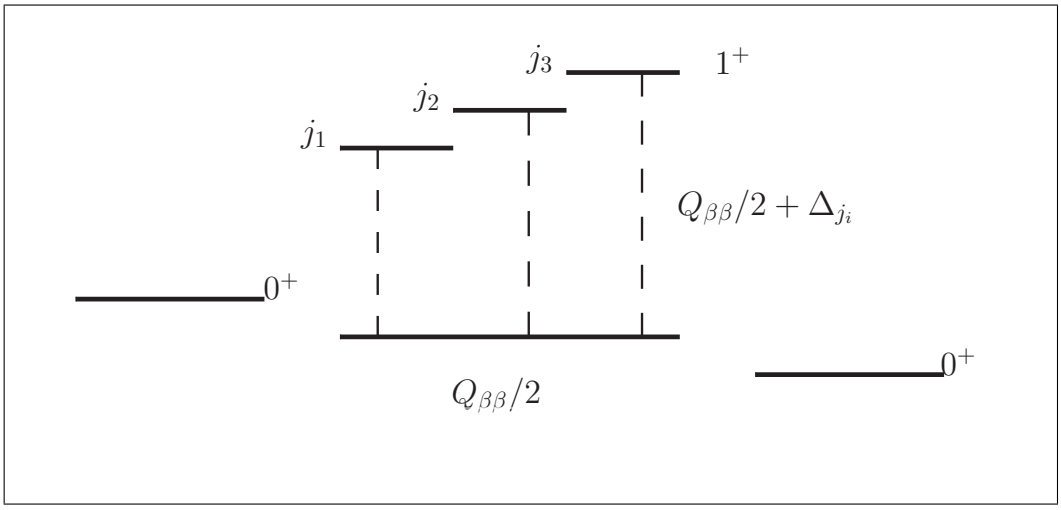

Figure 6: Generalized schematic for the weighing imposed to each of the intermediate levels. The average energy between initial and final states is added to the electron capture Q value of the various intermediate states. In the single state dominance hypothesis, only the lowest intermediate state affects the decay process

3.3.1 Example

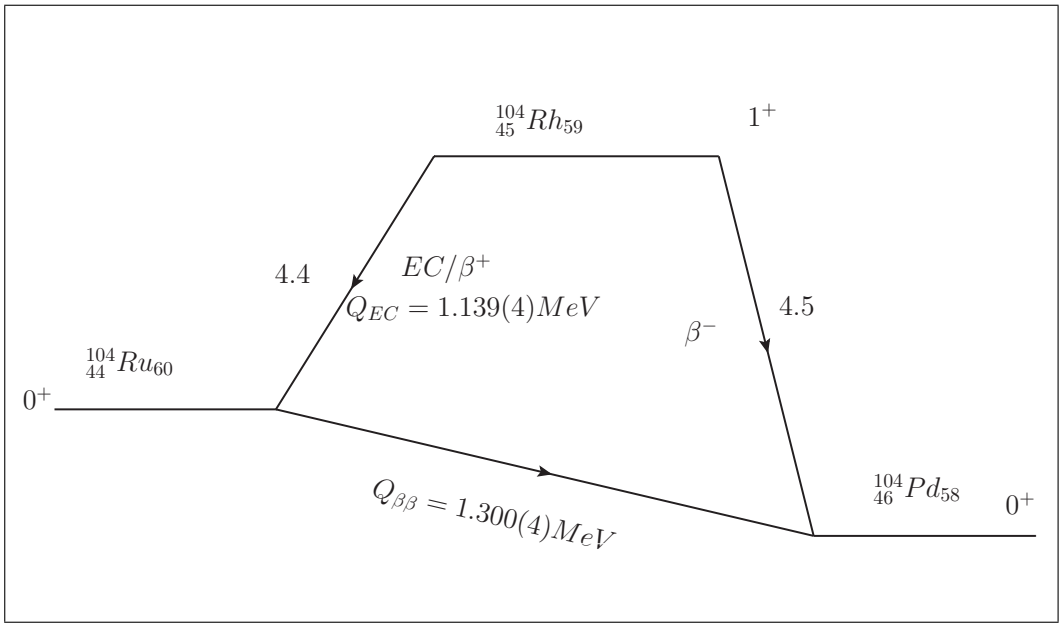

Figure 7: The structure of the double beta decay of Ru-104. Contains the relevant Q values and the experimental $\log ft$ values.

Consider the example case, where Ru-104 decays into Pd-104, as seen in figure 7. Now,

$$\begin{aligned} \Delta = Q_{ec} - m_e c^2 = 1.139 - 0.5109989 \approx 0.628 \\ Q_{\beta\beta} = 1.300. \end{aligned} \tag{63}$$

For a transition from the Ru-104 BCS-vacuum to the Pd-104 one, the matrix element can be determined using the single beta decay matrix elements calculated in 18 and 17

$$\begin{aligned} \left| M^{(2\nu)}_{DGT}(0^+ \to 0^+) \right| &= \left| \frac{2.0105 \cdot 2.8102}{(\frac{1.3}{2} + 0.628)/0.511 + 1} \right| \\ &= \left| \frac{5.64996}{3.501} \right| \approx 1.6138 \end{aligned} \tag{64}$$

The linear combination approximations from before can also be used here, by

considering a process

$$|BCS\rangle_1 \rightarrow \sum_i \alpha_i |\Psi_i\rangle \rightarrow |BCS\rangle_2. \tag{65}$$

The possible energy differences between the ground state and the linear combination are neglected. Tables 5 and 6 show the various approximation coefficients and the resulting $\left|M^{(2\nu)}_{DGT}\right|$ values for this case. Additionally, the process can also be

Table 5: Double beta matrix elements for the various two-level linear combinations that were calculated.

α_1	α_2	$M^{(2\nu)}_{DGT}$
0.614	0.789	0.273
0.888	0.459	0.446
0.345	0.939	0.271
0.074	-0.997	0.440

Table 6: Double beta matrix elements for the various three-level linear combinations calculated previously

α_1	α_2	α_3	$M^{(2\nu)}_{DGT}$
0.318	0.408	0.856	0.440
0.198	0.254	-0.947	0.383
0.287	0.148	0.947	0.383
0.173	0.089	-0.981	0.458
0.327	0.890	-0.318	0.119
0.247	0.672	-0.698	0.104
0.042	-0.566	0.823	0.041
0.062	-0.826	0.560	0.079

examined in a less rigorous fashion by requiring that each of the matrix elements in (61) reproduces the corresponding experimental result, i.e. use two separate approximations instead of one. In this case $\left|M^{(2\nu)}_{DGT}\right| = 0.116$. This is equivalent to calculating the matrix elements from their respective experimental $\log ft$ values.

4 Additional results

This section contains the results for the other decay processes examined. Each section contains a schematic for the process, the relevant BCS states, the single and double beta decay results and the linear combination coefficients used in approximations. The coefficients were used to calculate the log ft value for the process that was not used as a boundary condition and for the sake of easy comparison, the corresponding experimental value is also presented, see for example table 9. For the double beta case, the value based on the experimental results is based on using the same calculations used at the end of the previous section.

4.1 Zn-70 to Ge-70

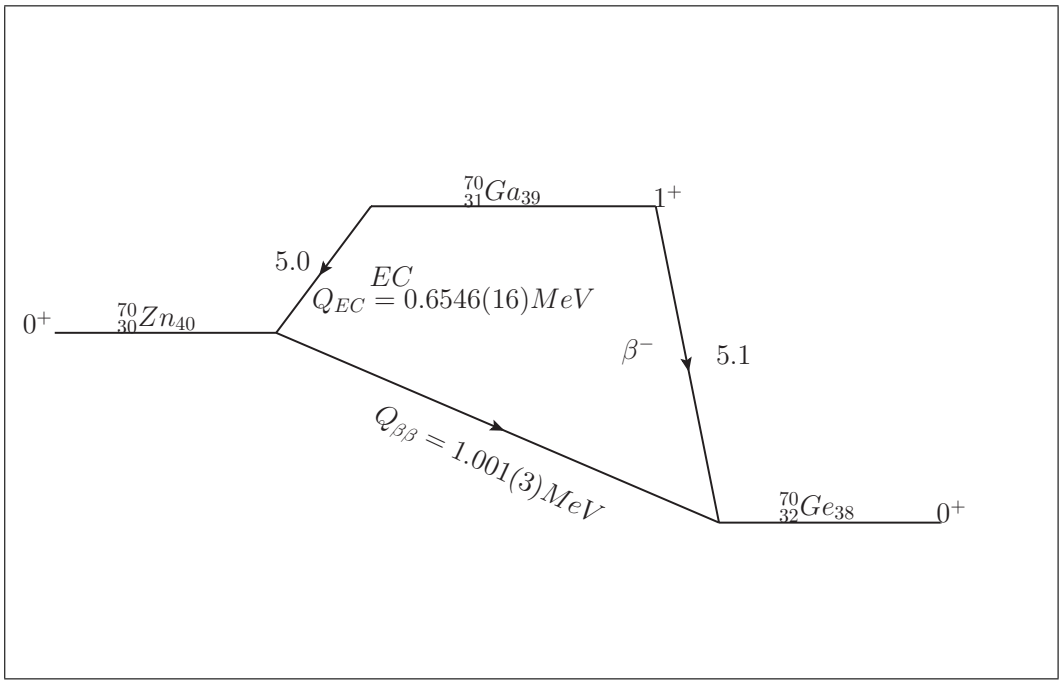

Figure 8: The decay process for Zn-70. The Q value of the decay is the second highest outside of the example case of Ru-104. The in-between nucleus is more stable than in any of the other processes being examined.

Proton	Neutron
$(1p_{\frac{3}{2}}, u = 0.80294)$	$(1p_{\frac{1}{2}}, v = 0.97472)$
$(0f_{\frac{5}{2}}, u = 0.96154)$	$(0f_{\frac{5}{2}}, v = 0.98386)$
$(1p_{\frac{1}{2}}, u = 0.9726)$	$(1p_{\frac{1}{2}}, v = 0.97472)$

Table 7: The zinc-70 proton and neutron state combinations with the lowest energy

Proton	Neutron
$(1p_{\frac{3}{2}} v = 0.76969)$,	$(1p_{\frac{1}{2}}, u = 0.63713])$
$(0f_{\frac{5}{2}}, v = 0.45956)$,	$(0f_{\frac{5}{2}}, u = 0.49828)$
$(1p_{\frac{1}{2}}, v = 0.33823)$,	$(1p_{\frac{1}{2}}, u = 0.63713)$

Table 8: The germanium-70 proton and neutron state combinations that correspond to the zinc states

The BCS predictions for the beta decays of gallium-70 are $\log ft = 3.544$ for β^+ and $\log ft = 3.950$ for β^-. The corresponding experimental values are $\log ft = 5.0$ and $\log ft = 5.1$

α_1	α_2	$\log ft$	$\log ft_{experimental}$
0.643	-0.766	4.934	5.1
0.815	-0.579	4.435	5.1
0.148	-0.989	3.613	5.0
0.601	-0.799	4.696	5.0

Table 9: Two state approximation for Ga-70

Previous α	α_1	α_2	α_3	$\log ft$	$\log ft_{experimental}$
(0.64,-0.77)	0.244	-0.291	0.925	4.520	5.0
(0.64,-0.77)	0.617	-0.736	-0.279	4.592	5.0
(0.81,-0.58)	0.162	-0.115	0.980	4.224	5.0
(0.81,-0.58)	0.544	-0.387	-0.745	4.967	5.0
(0.15,-0.99)	0.086	-0.574	0.815	7.061	5.1
(0.15,-0.99)	0.036	-0.244	0.969	6.092	5.1
(0.6,-0.8)	0.592	-0.787	0.174	5.028	5.1
(0.6,-0.8)	0.357	-0.474	0.805	5.047	5.1

Table 10: Three state approximation for Ga-70

BCS double beta decay matrix element $M_{\beta\beta} = 0.906$. The value based on experimental results is $M_{\beta\beta} = 0.045$.

α_1	α_2	$M_{\beta\beta}$
0.643	-0.766	0.055
0.815	-0.579	0.097
0.148	-0.989	0.223
0.601	-0.799	0.064

Table 11: Two state approximation for the double beta decay of Zn-70

α_1	α_2	α_3	$M_{\beta\beta}$
0.244	-0.291	0.925	0.078
0.617	-0.736	-0.279	0.072
0.162	-0.115	0.980	0.110
0.544	-0.387	-0.745	0.047
0.086	-0.574	0.815	0.005
0.036	-0.244	0.969	0.014
0.592	-0.787	0.174	0.049
0.357	-0.474	0.805	0.048

Table 12: Three state approximation for Zn-70 double beta decay

4.2 Se-80 to Kr-80

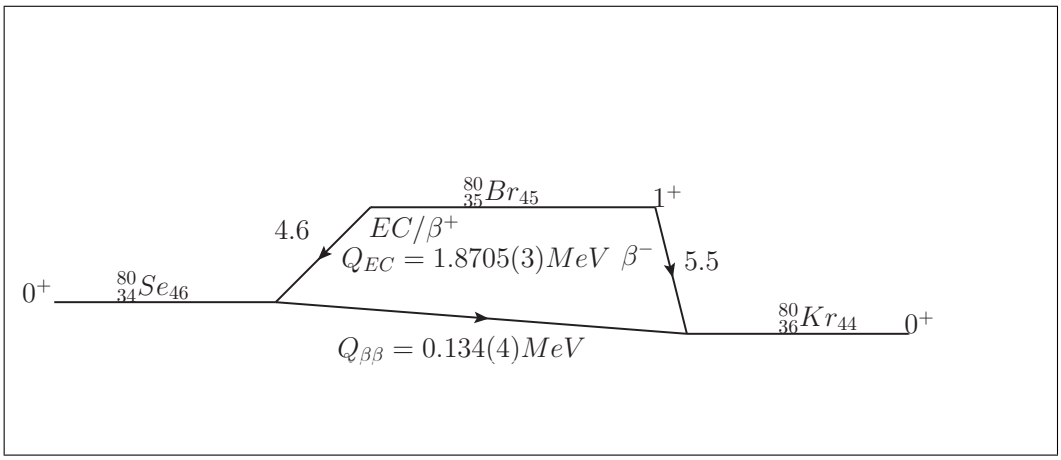

Figure 9: The decay process for Se-80. Note the extremely low Q value for the double beta decay. Experimental $logft$ for the single decays are dissimilar by a factor of almost 10.

Proton	Neutron
$(0g_{\frac{9}{2}}, u = 0.97665)$	$(0g_{\frac{9}{2}}, v = 0.79317)$
$(1p_{\frac{3}{2}}, u = 0.60435)$	$(1p_{\frac{1}{2}}, v = 0.96279)$
$(1p_{\frac{1}{2}}, u = 0.91965)$	$(1p_{\frac{1}{2}}, v = 0.96279)$

Table 13: Selenium-80 proton and neutron states to be combined

Proton	Neutron
$(0g_{\frac{9}{2}}, v = 0.26459)$,	$(0g_{\frac{9}{2}}, u = 0.729))$
$(1p_{\frac{3}{2}}, v = 0.8627)$,	$(1p_{\frac{1}{2}}, u = 0.34682)$
$(1p_{\frac{1}{2}}, v = 0.51641)$,	$(1p_{\frac{1}{2}}, u = 0.34682)$

Table 14: Krypton-80 proton and neutron states to be combined

The BCS predictions for the beta decays of bromine-80 are $\log ft = 3.193$ for β^+ and $\log ft = 4.4$ for β^-. The corresponding experimental values are $\log ft = 4.6$ and $\log ft = 5.5$

α_1	α_2	$\log ft$	$\log ft_{experimental}$
0.596	0.803	5.691	5.5
0.279	0.960	4.703	5.5
0.839	0.544	3.682	4.6
0.564	0.826	4.815	4.6

Table 15: Two state approximation for Br-80

(Previous α)	α_1	α_2	α_3	$\log ft$	$\log ft_{experimental}$
(0.6,0.8)	0.207	0.279	0.938	4.674	4.6
(0.6,0.8)	0.568	0.764	0.307	5.138	4.6
(0.28,0.96)	0.026	0.090	0.996	4.285	4.6
(0.28,0.96)	0.177	0.612	-0.771	5.388	4.6
(0.84,0.54)	0.577	0.374	0.726	7.275	5.5
(0.84,0.54)	0.099	0.064	0.993	5.880	5.5
(0.56,0.83)	0.556	0.813	-0.171	5.638	5.5
(0.56,0.83)	0.193	0.283	0.939	5.445	5.5

Table 16: Three state approximation for Br-80

BCS double beta decay matrix element $M_{\beta\beta} = 0.482$. The value based on experimental results is $M_{\beta\beta} = 0.027$.

α_1	α_2	$M_{\beta\beta}$
0.596	0.803	0.022
0.279	0.960	0.067
0.839	0.544	0.077
0.564	0.826	0.021

Table 17: Two state approximation for the double beta decay of Se-80

α_1	α_2	α_3	$M_{\beta\beta}$
0.207	0.279	0.938	0.025
0.568	0.764	0.307	0.014
0.026	0.090	0.996	0.039
0.177	0.612	-0.771	0.011
0.577	0.374	0.726	0.003
0.099	0.064	0.993	0.017
0.556	0.813	-0.171	0.023
0.193	0.283	0.939	0.029

Table 18: Three state approximation for Se-80 double beta decay

4.3 Cd-114 to Sn-114

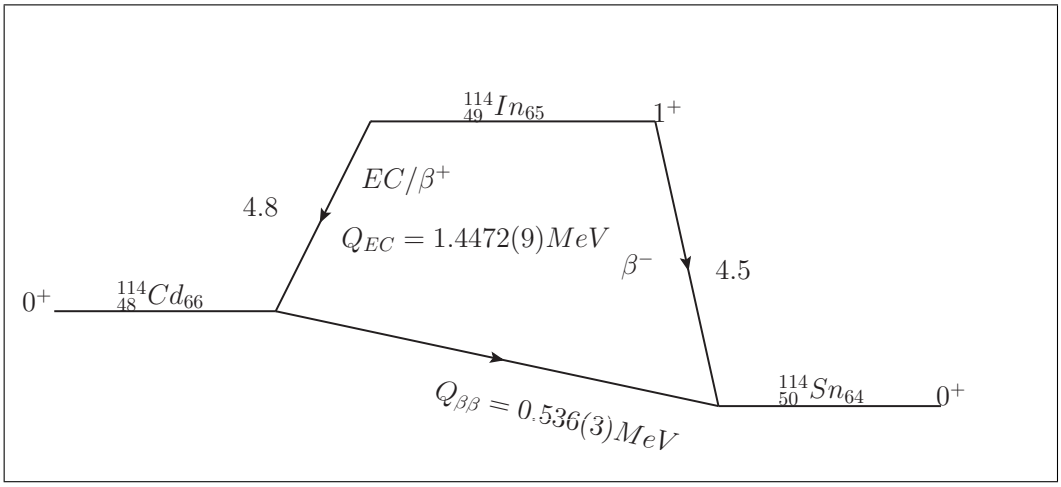

Figure 10: The decay process for Cd-114. There is some resemblance to the example case, but the double beta Q value is significantly lower. The log ft values imply a slightly slower process than the Ru-104 case, which the calculated matrix elements bear out.

Since tin has 50 protons, it has a full proton shell. Therefore the BCS-model does not lead to spreading of the proton states. Instead, as can be seen in table 20, the proton states have occupation amplitude of either 1 or 0, depending on the state.

Proton	Neutron
$(0g_{\frac{9}{2}}, u = 0.41651)$	$(0g_{\frac{7}{2}}, v = 0.91337)$
$(1d_{\frac{5}{2}}, u = 0.99623)$	$(1d_{\frac{3}{2}}, v = 0.59648)$
$(1d_{\frac{5}{2}}, u = 0.99623)$	$(1d_{\frac{5}{2}}, v = 0.95227)$

Table 19: Cadmium-114 proton and neutron states to be combined

Proton	Neutron
$(0g_{\frac{9}{2}}, v = 0.99998)$,	$(0g_{\frac{7}{2}}, u = 0.47281)$
$(1d_{\frac{5}{2}}, v = 0.0059)$,	$(1d_{\frac{3}{2}}, u = 0.88439)$
$(1d_{\frac{5}{2}}, v = 0.0059)$,	$(1d_{\frac{5}{2}}, u = 0.34535)$

Table 20: Tin-114 proton and neutron states to be combined

The BCS predictions for the beta decays of Indium-114 are $\log ft = 3.648$ for β^+ and $\log ft = 3.459$ for β^-. The corresponding experimental values are $\log ft = 4.8$ and $\log ft = 4.5$

α_1	α_2	$\log ft$	$\log ft_{experimental}$
0.628	-0.778	3.872	4.5
0.857	-0.515	3.597	4.5
0.294	0.956	3.361	4.8
0.309	-0.951	3.861	4.8

Table 21: Two state approximation for In-114

(Previous α)	α_1	α_2	α_3	$\log ft$	$\log ft_{experimental}$
(0.63,-0.78)	0.307	-0.381	0.872	3.226	4.8
(0.63,-0.78)	0.302	-0.374	-0.877	3.371	4.8
(0.86,-0.52)	0.306	-0.184	0.934	3.292	4.8
(0.86,-0.52)	0.300	-0.181	-0.937	3.188	4.8
(0.29,0.96)	0.204	0.664	0.719	4.825	4.5
(0.29,0.96)	0.249	0.809	0.532	4.650	4.5
(0.31,-0.95)	0.297	-0.912	-0.283	4.534	4.5
(0.31,-0.95)	0.261	-0.801	-0.539	4.644	4.5

Table 22: Three state approximation for In-114

BCS double beta decay matrix element $M_{\beta\beta} = 0.953$. The value based on experimental results is $M_{\beta\beta} = 0.076$.

α_1	α_2	$M_{\beta\beta}$
0.628	-0.778	0.157
0.857	-0.515	0.216
0.294	0.956	0.400
0.309	-0.951	0.225

Table 23: Two state approximation for the double beta decay of Cd-114

α_1	α_2	α_3	$M_{\beta\beta}$
0.307	-0.381	0.872	0.467
0.302	-0.374	-0.877	0.395
0.306	-0.184	0.934	0.433
0.300	-0.181	-0.937	0.488
0.204	0.664	0.719	0.052
0.249	0.809	0.532	0.064
0.297	-0.912	-0.283	0.073
0.261	-0.801	-0.539	0.065

Table 24: Three state approximation for Cd-114 double beta decay

5 Conclusions

Equations (66)-(69) contain the main results for each of the processes. There are four values given to the double beta matrix element; the value predicted by the BCS method in use, the effective value based on the experimental results of the corresponding single decays, and the best values based on the two- and three-state

linear approximations.

$$
\begin{aligned}
&\text{Zn-70} \rightarrow \text{Ge-70} \\
&M_{BCS} = 0.906, M_{eff} = 0.045 \\
&\text{Best approximations:} \\
&|pn1\rangle = 0.643|p : 1p_{\frac{3}{2}}, n : 1p_{\frac{1}{2}}\rangle - 0.766|p : 0f_{\frac{5}{2}}, n : 0f_{\frac{5}{2}}\rangle \\
&|pn1\rangle = 0.544|p : 1p_{\frac{3}{2}}, n : 1p_{\frac{1}{2}}\rangle - 0.387|p : 0f_{\frac{5}{2}}, n : 0f_{\frac{5}{2}}\rangle - 0.745|p : 1p_{\frac{1}{2}}, n : 1p_{\frac{1}{2}}\rangle \\
&M_{2\alpha} = 0.055, M_{3\alpha} = 0.047
\end{aligned}
\tag{66}
$$

$$
\begin{aligned}
&\text{Se-80} \rightarrow \text{Kr-80} \\
&M_{BCS} = 0.482, M_{eff} = 0.027 \\
&\text{Best approximations:} \\
&|pn1\rangle = 0.596|P : 0g_{\frac{9}{2}}, n : 0g_{\frac{9}{2}}\rangle + 0.803|p : 1p_{\frac{3}{2}}, n : 1p_{\frac{1}{2}}\rangle \\
&|pn1\rangle = 0.207|P : 0g_{\frac{9}{2}}, n : 0g_{\frac{9}{2}}\rangle + 0.279|p : 1p_{\frac{3}{2}}, n : 1p_{\frac{1}{2}}\rangle + 0.938|p : 1p_{\frac{1}{2}}, n : 1p_{\frac{1}{2}}\rangle \\
&M_{2\alpha} = 0.022, M_{3\alpha} = 0.025
\end{aligned}
\tag{67}
$$

$$
\begin{aligned}
&\text{Ru-104} \rightarrow \text{Pd-104} \\
&M_{BCS} = 1.614, M_{eff} = 0.116 \\
&\text{Best approximations:} \\
&|pn1\rangle = 0.345|p : 0g_{\frac{9}{2}}, n : 0g_{\frac{7}{2}}\rangle + 0.939|p : 0g_{\frac{9}{2}}, n : 0g_{\frac{9}{2}}\rangle \\
&|pn1\rangle = 0.327|p : 0g_{\frac{9}{2}}, n : 0g_{\frac{7}{2}}\rangle + 0.890|p : 0g_{\frac{9}{2}}, n : 0g_{\frac{9}{2}}\rangle - 0.318|p : 1d_{\frac{5}{2}} n : 1d_{\frac{5}{2}}\rangle \\
&M_{2\alpha} = 0.271, M_{3\alpha} = 0.119
\end{aligned}
\tag{68}
$$

$$
\begin{aligned}
&\text{Cd-114} \rightarrow \text{Su-114} \\
&M_{BCS} = 0.953, M_{eff} = 0.076 \\
&\text{Best approximations:} \\
&|pn1\rangle = 0.628|p : 0g_{\frac{9}{2}}, n : 0g_{\frac{7}{2}}\rangle - 0.778|p : 1d_{\frac{5}{2}}, n : 1d_{\frac{3}{2}}\rangle \\
&|pn1\rangle = 0.297|p : 0g_{\frac{9}{2}}, n : 0g_{\frac{7}{2}}\rangle - 0.912|p : 1d_{\frac{5}{2}}, n : 1d_{\frac{3}{2}}\rangle - 0.283|p : 1d_{\frac{5}{2}}, n : 1d_{\frac{5}{2}}\rangle \\
&M_{2\alpha} = 0.157, M_{3\alpha} = 0.073
\end{aligned}
\tag{69}
$$

It is clear from the above, that the BCS model needs to be extended to account for quasiparticle interactions, and that these interactions lead to a slower decay process. The magnitude of the deviation between the BCS and effective values is explained by remembering that the double decay is a composite of two single beta decays. The difference between experimental and BCS matrix elements is inherited by the double beta decay matrix element. This leads to the BCS results being more than ten times larger than the effective value.

What of the linear combination method that I tried to use to address this? Since one of the single decay processes is used as a boundary condition, the double beta decay matrix element approaches the effective value. Since one of the processes is not bounded, there will almost invariably be some difference between the values. For these values to be the simultaneously correct, the quasiparticle excitations in the initial and final BCS vacuums would have to account for the difference in $\log ft$. As such, the use of linear combinations should be treated as a crude approximation at most.

The structure of the linear combinations can be divided into two types: those with only positive coefficients and those with one or more negative coefficients. The negative coefficients imply a sort of resistive influence on the process. This is likely due to the boundary condition, the single decay experimental values, being too slow to be caused by any of the proton-neutron states being used in the combination. A negative coefficient reduces the absolute value of the matrix element, slowing the decay process. The positive coefficients, on the other hand, produce superpositions of quasiparticle states that decay slow enough to be comparable to the experimental results.

Overall, the results have a certain consistency about them; if a process is predicted

to be faster in the BCS model, it is estimated to be faster in every approximation. One should note, however, that the linear combinations do not produce correct $\log ft$ values for the process that was not used as a boundary condition. Generally, the $\log ft$ values swing wildly about their expected values, with the best double beta results being those closest to the experimental values.

The results presented in this study can be used to evaluate which process might be relevant to the search for neutrinoless double beta decay. Since a larger matrix element corresponds to a larger $\log ft$ term, the best choice would have the largest matrix element. If the matrix element was the sole determining factor, the order of experimental relevance would be: Ru-104, Cd-114, Zn-70 and Se-80. The order is not final, since this study did not include calculating the phase space for these processes. Furthermore, experimental considerations would also have to include, for example, the preparation of the isotope; since the process is slow, a large amount of the isotope should be prepared. The Q value of the decay process is also relevant, as the neutrinoless decay can only be measured by observing the energy of the electrons and comparing it to the Q value. See for example [12] or [13] for some details on the ongoing experiments.

These results show that additional work needs to be done to reach accurate values for the double beta decay matrix element. There is a clear difference between the BCS and the expected matrix elements. The continuation of this work is thus divided into two parts: determining the phase space f for each of the processes and correcting the BCS results by adding in the residual interactions not accounted for in this study. This will lead to a improved matrix element which can be used to determine the half-life of each of the isotopes that were examined here. These results can then be used to determine if these isotopes are useful in looking for neutrinoless double beta decay.

References

[1] J. Suhonen. *From Nucleons to Nucleus: Concepts of Microscopic Nuclear Theory*. Theoretical and Mathematical Physics. Springer Berlin Heidelberg, 2007.

[2] John Bardeen, Leon N Cooper, and John Robert Schrieffer. Theory of superconductivity. *Physical Review*, 108(5):1175, 1957.

[3] A. Bohr, B. R. Mottelson, and D. Pines. Possible analogy between the excitation spectra of nuclei and those of the superconducting metallic state. *Phys. Rev.*, 110:936–938, May 1958.

[4] R.A. Broglia and V. Zelevinsky. *Fifty Years of Nuclear BCS: Pairing in Finite Systems*. World Scientific, 2013.

[5] D. J. Dean and M. Hjorth-Jensen. Pairing in nuclear systems: from neutron stars to finite nuclei. *Rev. Mod. Phys.*, 75:607–656, Apr 2003.

[6] M. Wang, G. Audi, A.H. Wapstra, F.G. Kondev, M. MacCormick, X. Xu, and B. Pfeiffer. The ame2012 atomic mass evaluation. *Chinese Physics C*, 36(12):1603, 2012.

[7] R. Casten. *Nuclear structure from a simple perspective*. Oxford studies in nuclear physics. Oxford University Press, New York, 1990.

[8] Evaluated nuclear structure data file search and retrieval. `https://www.nndc.bnl.gov/ensdf/`. Accessed: September 14 2018.

[9] Kai Zuber. *Neutrino Physics*. Series in High Energy Physics, Cosmology and Gravitation. IOP Publishing, 2004.

[10] O. Civitarese and J. Suhonen. Is the single-state dominance realized in double-β-decay transitions? *Phys. Rev. C*, 58:1535–1538, Sep 1998.

[11] Interactive chart of nuclides. `https://www.nndc.bnl.gov/chart/`. Accessed: May 14 2018.

[12] Reyco Henning. Current status of neutrinoless double-beta decay searches. *Reviews in Physics*, 1:29–35, 2016.

[13] Oliviero Cremonesi. Experimental searches of neutrinoless double beta decay. *Nuclear Physics B-Proceedings Supplements*, 237:7–12, 2013.

A Angular momentum coupling

This section shows how to calculate the Wigner 6J-symbol used in (16).

A.1 Clebsch-Gordan coefficients

Start with the following case:

$$|1,0\rangle = a|\frac{1}{2}\,\frac{1}{2}\rangle|\frac{1}{2}\;-\frac{1}{2}\rangle + b|\frac{1}{2}\;-\frac{1}{2}\rangle|\frac{1}{2}\,\frac{1}{2}\rangle. \tag{70}$$

Now

$$J^2|1\,0\rangle = 2|1\,0\rangle. \tag{71}$$

On the other hand

$$J^2 = J_1^2 + J_2^2 + 2J_1 \cdot J_2 = J_1^2 + J_2^2 + 2J_{1z}J_{2z} + J_{1+}J_{2-} + J_{1-}J_{2+}. \tag{72}$$

Inserting (72) and (70) into (71) leads to

$$\begin{aligned}
J^2|1,0\rangle &= a(\frac{1}{2}(\frac{1}{2}+1) + \frac{1}{2}(\frac{1}{2}+1) - 2\cdot\frac{1}{2}\frac{1}{2})|\frac{1}{2}\,\frac{1}{2}\rangle|\frac{1}{2}\;-\frac{1}{2}\rangle \\
&+ b(\frac{1}{2}(\frac{1}{2}+1) + \frac{1}{2}(\frac{1}{2}+1) - \frac{1}{2})|\frac{1}{2}\;-\frac{1}{2}\rangle|\frac{1}{2}\,\frac{1}{2}\rangle \\
&+ a\sqrt{\left[\frac{1}{2}(\frac{1}{2}+1) - \frac{1}{2}(\frac{1}{2}-1)\right]\cdot\left[\frac{1}{2}(\frac{1}{2}+1) + \frac{1}{2}(1-\frac{1}{2})\right]}|\frac{1}{2}\,\frac{1}{2}\rangle|\frac{1}{2}\;-\frac{1}{2}\rangle \\
&+ b\sqrt{\left[\frac{1}{2}(\frac{1}{2}+1) + \frac{1}{2}(1-\frac{1}{2})\right]\cdot\left[\frac{1}{2}(\frac{1}{2}+1) - \frac{1}{2}(\frac{1}{2}-1)\right]}|\frac{1}{2}\;-\frac{1}{2}\rangle|\frac{1}{2}\,\frac{1}{2}\rangle \\
&= (a\left[\frac{3}{4}+\frac{3}{4}-\frac{1}{2}\right] + b\sqrt{(\frac{3}{4}+\frac{1}{4})\cdot(\frac{3}{4}+\frac{1}{4})})|\frac{1}{2}\,\frac{1}{2}\rangle|\frac{1}{2}\;-\frac{1}{2}\rangle \\
&+ (b\left[\frac{3}{4}+\frac{3}{4}-\frac{1}{2}\right] + a\sqrt{(\frac{3}{4}+\frac{1}{4})\cdot(\frac{3}{4}+\frac{1}{4})})|\frac{1}{2}\;-\frac{1}{2}\rangle|\frac{1}{2}\,\frac{1}{2}\rangle \\
&= (a+b)|\frac{1}{2}\,\frac{1}{2}\rangle|\frac{1}{2}\;-\frac{1}{2}\rangle + (a+b)|\frac{1}{2}\;-\frac{1}{2}\rangle|\frac{1}{2}\,\frac{1}{2}\rangle
\end{aligned} \tag{73}$$

Inserting (71) combined with (70) to the left leads to

$$2a = a + b \Rightarrow a = b. \tag{74}$$

Since the coefficients are normalized, (74) leads to

$$2a^2 = 1 \Rightarrow a = \frac{1}{\sqrt{2}}. \tag{75}$$

Therefore the Clebsch-Gordan coefficents are

$$\left(\frac{1}{2}\,\frac{1}{2}\,\frac{1}{2}\;-\frac{1}{2}|1\,0\right) = \left(\frac{1}{2}\;-\frac{1}{2}\,\frac{1}{2}\,\frac{1}{2}|1\,0\right) = \frac{1}{\sqrt{2}} \tag{76}$$

B Wigner 3J- and 6J-symbols

The Clebsch-Gordan coefficients are connected to the Wigner 3J-symbols by

$$\begin{pmatrix} j_1 & j_2 & j_3 \\ m_1 & m_2 & m_3 \end{pmatrix} = (-1)^{j_1 - j_2 - m_3} \frac{1}{\sqrt{2j_3 + 1}} \left(j_1\, m_1\, j_2\, m_2 | j_3\; -m_3\right) \tag{77}$$

Therefore

$$\begin{aligned} \begin{pmatrix} \frac{1}{2} & \frac{1}{2} & 1 \\ \frac{1}{2} & -\frac{1}{2} & 0 \end{pmatrix} &= (-1)^{\frac{1}{2} - \frac{1}{2} - 0} \frac{1}{\sqrt{2+1}} \left(\frac{1}{2}\,\frac{1}{2}\,\frac{1}{2}\;-\frac{1}{2}|1\,0\right) \\ &= \frac{1}{\sqrt{3}} \cdot \frac{1}{\sqrt{2}} = \frac{1}{\sqrt{6}}. \end{aligned} \tag{78}$$

The following property of the Wigner 3J-symbols is used later:

$$\begin{pmatrix} j_1 & j_2 & j_3 \\ m_1 & m_2 & m_3 \end{pmatrix} = (-1)^{j_1 + j_2 + j_3} \begin{pmatrix} j_2 & j_1 & j_3 \\ m_2 & m_1 & m_3 \end{pmatrix}. \tag{79}$$

The Wigner 3J-symbol is related to the Wigner 6J-symbol by

$$\begin{Bmatrix} j_1 & j_2 & j_{12} \\ j_3 & j & j_{23} \end{Bmatrix} = \sum_{\substack{m_1 m_2 m_3 \\ m_{12} m_{23} m}} (-1)^{j_3+j+j_{23}-m_3-m-m_{23}} \begin{pmatrix} j_1 & j_2 & j_{12} \\ m_1 & m_2 & m_{12} \end{pmatrix} \times \begin{pmatrix} j_1 & j & j_{23} \\ m_1 & -m & m_{23} \end{pmatrix} \begin{pmatrix} j_3 & j_2 & j_{23} \\ m_3 & m_2 & -m_{23} \end{pmatrix} \begin{pmatrix} j_3 & j & j_{12} \\ -m_3 & m & m_{12} \end{pmatrix} \tag{80}$$

The 6J-symbol to be calculated is

$$\begin{Bmatrix} \frac{1}{2} & \frac{1}{2} & 1 \\ \frac{9}{2} & \frac{7}{2} & 4 \end{Bmatrix} = \sum_{\substack{m_1 m_2 m_3 \\ m_{12} m_{23} m}} (-1)^{12-m3_3-m-m_{23}} \begin{pmatrix} \frac{1}{2} & \frac{1}{2} & 1 \\ m_1 & m_2 & m_{12} \end{pmatrix} \times \begin{pmatrix} \frac{1}{2} & \frac{7}{2} & 4 \\ m_1 & -m & m_{23} \end{pmatrix} \begin{pmatrix} \frac{9}{2} & \frac{1}{2} & 4 \\ m_3 & m_2 & -m_{23} \end{pmatrix} \begin{pmatrix} \frac{9}{2} & \frac{7}{2} & 1 \\ -m_3 & m & m_{12} \end{pmatrix} \tag{81}$$

The first Wigner 3J-symbol has four possible variations for the different m values For $m_{12} = \pm 1$ the value of the symbol is $\frac{-1}{\sqrt{3}}$, and the $m_{12} = \pm 0$ case has already been calculated to be $\frac{1}{\sqrt{6}}$. Split the equation into four parts, named A,B,C and D. Now,

$$A = (-1)^{12-3m+\frac{3}{2}}(-\frac{1}{\sqrt{3}}) \begin{pmatrix} \frac{1}{2} & \frac{7}{2} & 4 \\ \frac{1}{2} & -m & m-\frac{1}{2} \end{pmatrix} \begin{pmatrix} \frac{9}{2} & \frac{1}{2} & 4 \\ m-1 & \frac{1}{2} & \frac{1}{2}-m \end{pmatrix} \times \begin{pmatrix} \frac{9}{2} & \frac{7}{2} & 1 \\ 1-m & m & -1 \end{pmatrix}, \tag{82}$$

where the spin numbers were determined by requiring $m_a + m_b + m_c = 0$ for the spin numbers in each 3J-symbol, as otherwise the value of the symbol is 0. Now,

$$\begin{aligned}
B &= (-1)^{12-3m-\frac{3}{2}}(-\frac{1}{\sqrt{3}})\begin{pmatrix} \frac{1}{2} & \frac{7}{2} & 4 \\ -\frac{1}{2} & -m & m+\frac{1}{2} \end{pmatrix}\begin{pmatrix} \frac{9}{2} & \frac{1}{2} & 4 \\ m+1 & -\frac{1}{2} & -(m+\frac{1}{2}) \end{pmatrix} \\
&\times \begin{pmatrix} \frac{9}{2} & \frac{7}{2} & 1 \\ -(m+1) & m & 1 \end{pmatrix} \\
&= (-1)^{12-3m-\frac{3}{2}}(-\frac{1}{\sqrt{3}})\begin{pmatrix} \frac{1}{2} & \frac{7}{2} & 4 \\ \frac{1}{2} & m & -m-\frac{1}{2} \end{pmatrix}(-1)\begin{pmatrix} \frac{9}{2} & \frac{1}{2} & 4 \\ -(m+1) & \frac{1}{2} & (m+\frac{1}{2}) \end{pmatrix} \\
&\times (-1)\begin{pmatrix} \frac{9}{2} & \frac{7}{2} & 1 \\ m+1 & -m & -1 \end{pmatrix} \\
&= (-1)^{12+3m+\frac{1}{2}}(-\frac{1}{\sqrt{3}})\begin{pmatrix} \frac{1}{2} & \frac{7}{2} & 4 \\ \frac{1}{2} & -m & m-\frac{1}{2} \end{pmatrix}\begin{pmatrix} \frac{9}{2} & \frac{1}{2} & 4 \\ m-1 & \frac{1}{2} & \frac{1}{2}-m \end{pmatrix} \\
&\times \begin{pmatrix} \frac{9}{2} & \frac{7}{2} & 1 \\ 1-m & m & -1 \end{pmatrix},
\end{aligned} \tag{83}$$

where the last step is done by changing summation index from m to -m. A and B are now exceedingly similar, the power expected. However

$$\begin{aligned}
12 - 3m + \frac{3}{2} &= 12 - (3m + \frac{1}{2}) + \frac{4}{2} = 14 - k \\
12 + 3m + \frac{1}{2} &= 12 + (3m + \frac{1}{2}) = 12 + k,
\end{aligned} \tag{84}$$

i.e. both powers are mutually odd or even, so the A and B terms never cancel each other out. Therefore

$$\begin{aligned}
A + B = (-1)^{12+3m+\frac{3}{2}}(\frac{2}{\sqrt{3}})&\begin{pmatrix} \frac{1}{2} & \frac{7}{2} & 4 \\ \frac{1}{2} & -m & m-\frac{1}{2} \end{pmatrix}\begin{pmatrix} \frac{9}{2} & \frac{1}{2} & 4 \\ m-1 & \frac{1}{2} & \frac{1}{2}-m \end{pmatrix} \\
&\times \begin{pmatrix} \frac{9}{2} & \frac{7}{2} & 1 \\ 1-m & m & -1 \end{pmatrix}.
\end{aligned} \tag{85}$$

The other two terms proceed similarly:

$$C = (-1)^{12-3m+\frac{1}{2}} \frac{1}{\sqrt{6}} \begin{pmatrix} \frac{1}{2} & \frac{7}{2} & 4 \\ \frac{1}{2} & -m & m-\frac{1}{2} \end{pmatrix} \begin{pmatrix} \frac{9}{2} & \frac{1}{2} & 4 \\ m & -\frac{1}{2} & \frac{1}{2}-m \end{pmatrix} \times \begin{pmatrix} \frac{9}{2} & \frac{7}{2} & 1 \\ -m & m & 0 \end{pmatrix}, \tag{86}$$

and

$$\begin{aligned} D &= (-1)^{12-3m-\frac{1}{2}} \frac{1}{\sqrt{6}} \begin{pmatrix} \frac{1}{2} & \frac{7}{2} & 4 \\ -\frac{1}{2} & -m & m\frac{1}{2} \end{pmatrix} \begin{pmatrix} \frac{9}{2} & \frac{1}{2} & 4 \\ m & \frac{1}{2} & -\frac{1}{2}-m \end{pmatrix} \\ &\times \begin{pmatrix} \frac{9}{2} & \frac{7}{2} & 1 \\ m & -m & 0 \end{pmatrix} \\ &= (-1)^{12+3m+\frac{3}{2}} \frac{1}{\sqrt{6}} \begin{pmatrix} \frac{1}{2} & \frac{7}{2} & 4 \\ \frac{1}{2} & -m & m-\frac{1}{2} \end{pmatrix} \begin{pmatrix} \frac{9}{2} & \frac{1}{2} & 4 \\ m & -\frac{1}{2} & \frac{1}{2}-m \end{pmatrix} \\ &\times \begin{pmatrix} \frac{9}{2} & \frac{7}{2} & 1 \\ -m & m & 0 \end{pmatrix}, \end{aligned} \tag{87}$$

and therefore

$$C + D = (-1)^{12-3m+\frac{1}{2}} \frac{2}{\sqrt{6}} \begin{pmatrix} \frac{1}{2} & \frac{7}{2} & 4 \\ \frac{1}{2} & -m & m-\frac{1}{2} \end{pmatrix} \begin{pmatrix} \frac{9}{2} & \frac{1}{2} & 4 \\ m & -\frac{1}{2} & \frac{1}{2}-m \end{pmatrix} \times \begin{pmatrix} \frac{9}{2} & \frac{7}{2} & 1 \\ -m & m & 0 \end{pmatrix}. \tag{88}$$

Inserting (85) and (88) into (81) leads to

$$\begin{aligned} \begin{Bmatrix} \frac{1}{2} & \frac{1}{2} & 1 \\ \frac{9}{2} & \frac{7}{2} & 4 \end{Bmatrix} &= \sum_{m=-\frac{7}{2}}^{\frac{7}{2}} (-1)^{12+3m+\frac{3}{2}} \begin{pmatrix} \frac{1}{2} & \frac{7}{2} & 4 \\ \frac{1}{2} & -m & m-\frac{1}{2} \end{pmatrix} \\ &\times \Big((\frac{2}{\sqrt{3}}) \begin{pmatrix} \frac{9}{2} & \frac{1}{2} & 4 \\ m-1 & \frac{1}{2} & \frac{1}{2}-m \end{pmatrix} \begin{pmatrix} \frac{9}{2} & \frac{7}{2} & 1 \\ 1-m & m & -1 \end{pmatrix} \\ &+ \frac{2}{\sqrt{6}} \begin{pmatrix} \frac{9}{2} & \frac{1}{2} & 4 \\ m & -\frac{1}{2} & \frac{1}{2}-m \end{pmatrix} \begin{pmatrix} \frac{9}{2} & \frac{7}{2} & 1 \\ -m & m & 0 \end{pmatrix} \Big). \end{aligned} \tag{89}$$

The rest of the calculation is finding the value of each of the 3J-symbols. As there are a total of $8 \times 5 = 40$ 3J-symbols in the sum, I'll use a program to evaluate

the above sum numerically. The output of the program is -0.192450089729875 + 0.0342133492853112*I, where the imaginary component is a computing error caused by too small numbers. Checking the value of the original 6J-symbol, it is found to be $-\frac{3}{9} \approx -0.192450089729875$. Therefore (89) leads to the exact solution when it is correctly calculated by hand.

C BCS results

This section contains the BCS values for the rest of the nucleons.

C.1 A = 70

The pairing strength values for Zn-70 were determined to be $G_N = 0.99181$ and $G_P = 1.03177$

Table 25: Neutron state quantum numbers, occupation amplitudes and quasi-particle energies for Zn-70

State	u	v	E_{qp}
$1p_{\frac{1}{2}}$	0.22345	0.97472	1.52991
$1p_{\frac{3}{2}}$	0.10978	0.99396	3.27359
$0f_{\frac{5}{2}}$	0.17896	0.98386	2.17871
$0f_{\frac{7}{2}}$	0.04995	0.99875	7.24315
$2s_{\frac{1}{2}}$	0.99974	0.02289	5.98011
$1d_{\frac{3}{2}}$	0.99964	0.02682	7.48441
$1d_{\frac{5}{2}}$	0.99918	0.04060	5.07189
$0g_{\frac{7}{2}}$	0.99926	0.03855	8.76910
$0g_{\frac{9}{2}}$	0.98338	0.18156	1.63794
$0h_{\frac{11}{2}}$	0.99980	0.02015	10.39009

Table 26: Proton state quantum numbers, occupation amplitudes and quasi-particle energies for Zn-70

State	u	v	E_{qp}
$1p_{\frac{1}{2}}$	0.97260	0.23248	2.93090
$1p_{\frac{3}{2}}$	0.80294	0.59607	1.20265
$0f_{\frac{5}{2}}$	0.96154	0.27465	1.84153
$0f_{\frac{7}{2}}$	0.11166	0.99375	4.67149
$2s_{\frac{1}{2}}$	0.99987	0.01587	10.63085
$1d_{\frac{3}{2}}$	0.99962	0.02772	12.30574
$1d_{\frac{5}{2}}$	0.99943	0.03387	9.10044
$0g_{\frac{7}{2}}$	0.99948	0.03218	13.07499
$0g_{\frac{9}{2}}$	0.99535	0.09630	4.45650
$0h_{\frac{11}{2}}$	0.99974	0.02297	13.51674

The pairing strength values for Ge-70 were determined to be $G_N = 1.19413$ and $G_P = 1.01141$

Table 27: Neutron state quantum numbers, occupation amplitudes and quasi-particle energies for Ge-70

State	u	v	E_{qp}
$1p_{\frac{1}{2}}$	0.63713	0.77075	1.86397
$1p_{\frac{3}{2}}$	0.34868	0.93724	2.97521
$0f_{\frac{5}{2}}$	0.49828	0.86702	2.18838
$0f_{\frac{7}{2}}$	0.14806	0.98898	6.72657
$2s_{\frac{1}{2}}$	0.99891	0.04663	7.52273
$1d_{\frac{3}{2}}$	0.99829	0.05850	9.08450
$1d_{\frac{5}{2}}$	0.99617	0.08746	6.39946
$0g_{\frac{7}{2}}$	0.99669	0.08134	10.11363
$0g_{\frac{9}{2}}$	0.95830	0.28577	2.91852
$0h_{\frac{11}{2}}$	0.99876	0.04974	11.55482

Table 28: Proton state quantum numbers, occupation amplitudes and quasi-particle energies for Ge-70

State	u	v	E_{qp}
$1p_{\frac{1}{2}}$	0.94106	0.33823	2.40300
$1p_{\frac{3}{2}}$	0.63842	0.76969	1.45403
$0f_{\frac{5}{2}}$	0.88815	0.45956	1.53687
$0f_{\frac{7}{2}}$	0.13539	0.99079	5.29762
$2s_{\frac{1}{2}}$	0.99970	0.02462	9.20899
$1d_{\frac{3}{2}}$	0.99933	0.03671	10.95861
$1d_{\frac{5}{2}}$	0.99880	0.04894	8.06316
$0g_{\frac{7}{2}}$	0.99900	0.04464	12.08114
$0g_{\frac{9}{2}}$	0.98838	0.15202	3.84675
$0h_{\frac{11}{2}}$	0.99946	0.03291	12.61657

C.2 A=80

The pairing strength values for Se-80 were determined to be $G_N = 1.21517$ and $G_P = 1.04135$

Table 29: Neutron state quantum numbers, occupation amplitudes and quasi-particle energies for Se-80

State	u	v	E_{qp}
$1p_{\frac{1}{2}}$	0.27024	0.96279	3.57862
$1p_{\frac{3}{2}}$	0.17841	0.98396	5.06177
$0f_{\frac{5}{2}}$	0.24745	0.96890	4.73010
$0f_{\frac{7}{2}}$	0.10179	0.99481	8.95427
$2s_{\frac{1}{2}}$	0.99622	0.08689	4.91316
$1d_{\frac{3}{2}}$	0.99505	0.09941	6.21940
$1d_{\frac{5}{2}}$	0.98884	0.14900	3.69020
$0g_{\frac{7}{2}}$	0.98785	0.15539	6.60426
$0g_{\frac{9}{2}}$	0.60900	0.79317	1.54079
$0h_{\frac{11}{2}}$	0.99785	0.06550	8.28435

Table 30: Proton state quantum numbers, occupation amplitudes and quasi-particle energies for Se-80

State	u	v	E_{qp}
$1p_{\frac{1}{2}}$	0.91965	0.39274	2.40406
$1p_{\frac{3}{2}}$	0.60435	0.79672	1.73457
$0f_{\frac{5}{2}}$	0.72912	0.68439	1.56398
$0f_{\frac{7}{2}}$	0.15689	0.98762	5.67841
$2s_{\frac{1}{2}}$	0.99962	0.02755	10.15916
$1d_{\frac{3}{2}}$	0.99919	0.04035	11.52035
$1d_{\frac{5}{2}}$	0.99839	0.05674	8.23935
$0g_{\frac{7}{2}}$	0.99821	0.05980	11.20564
$0g_{\frac{9}{2}}$	0.97665	0.21484	3.38526
$0h_{\frac{11}{2}}$	0.99910	0.04235	11.96391

The pairing strength values for Kr-80 were determined to be $G_N = 1.26894$ and $G_P = 1.06289$

Table 31: Neutron state quantum numbers, occupation amplitudes and quasi-particle energies for Kr-80

State	u	v	E_{qp}
$1p_{\frac{1}{2}}$	0.34682	0.93793	3.25183
$1p_{\frac{3}{2}}$	0.22463	0.97444	4.68620
$0f_{\frac{5}{2}}$	0.30048	0.95379	4.43415
$0f_{\frac{7}{2}}$	0.12177	0.99256	8.62478
$2s_{\frac{1}{2}}$	0.99684	0.07948	5.84684
$1d_{\frac{3}{2}}$	0.99543	0.09552	7.15596
$1d_{\frac{5}{2}}$	0.99020	0.13968	4.44606
$0g_{\frac{7}{2}}$	0.98783	0.15551	7.36600
$0g_{\frac{9}{2}}$	0.72900	0.68451	1.70930
$0h_{\frac{11}{2}}$	0.99760	0.06923	8.94571

Table 32: Proton state quantum numbers, occupation amplitudes and quasi-particle energies for Kr-80

State	u	v	E_{qp}
$1p_{\frac{1}{2}}$	0.85634	0.51641	2.00962
$1p_{\frac{3}{2}}$	0.50572	0.86270	2.04317
$0f_{\frac{5}{2}}$	0.59687	0.80234	1.76133
$0f_{\frac{7}{2}}$	0.14919	0.98881	6.18277
$2s_{\frac{1}{2}}$	0.99944	0.03352	9.05898
$1d_{\frac{3}{2}}$	0.99890	0.04692	10.44144
$1d_{\frac{5}{2}}$	0.99769	0.06792	7.39105
$0g_{\frac{7}{2}}$	0.99752	0.07032	10.40105
$0g_{\frac{9}{2}}$	0.96436	0.26459	2.89569
$0h_{\frac{11}{2}}$	0.99888	0.04729	11.19060

C.3 A=114

The pairing strength values for Cd-114 were determined to be $G_N = 0.97716$ and $G_P = 1.07491$

Table 33: Neutron state quantum numbers, occupation amplitudes and quasi-particle energies for Cd-114

State	u	v	E_{qp}
$1p_{\frac{1}{2}}$	0.08884	0.99605	8.66883
$1p_{\frac{3}{2}}$	0.08147	0.99668	9.97001
$0f_{\frac{5}{2}}$	0.07055	0.99751	10.48913
$0f_{\frac{7}{2}}$	0.05701	0.99837	13.79410
$2s_{\frac{1}{2}}$	0.67396	0.73877	1.35153
$1d_{\frac{3}{2}}$	0.80263	0.59648	1.35380
$1d_{\frac{5}{2}}$	0.30527	0.95227	2.40931
$0g_{\frac{7}{2}}$	0.40714	0.91337	1.88234
$0g_{\frac{9}{2}}$	0.11083	0.99384	6.50748
$2p_{\frac{1}{2}}$	0.99917	0.04065	7.28700
$2p_{\frac{3}{2}}$	0.99887	0.04756	6.59505
$1f_{\frac{5}{2}}$	0.99870	0.05088	8.39570
$1f_{\frac{7}{2}}$	0.99659	0.08245	5.61270
$0h_{\frac{9}{2}}$	0.99733	0.07297	8.43672
$0h_{\frac{11}{2}}$	0.93737	0.34833	1.84426

Table 34: Proton state quantum numbers, occupation amplitudes and quasi-particle energies for Cd-114

State	u	v	E_{qp}
$1p_{\frac{1}{2}}$	0.29382	0.95586	2.31492
$1p_{\frac{3}{2}}$	0.17652	0.98430	3.70271
$0f_{\frac{5}{2}}$	0.17160	0.98517	4.50516
$0f_{\frac{7}{2}}$	0.07698	0.99703	8.34988
$2s_{\frac{1}{2}}$	0.99901	0.04444	6.93293
$1d_{\frac{3}{2}}$	0.99832	0.05798	7.45243
$1d_{\frac{5}{2}}$	0.99623	0.08681	4.65326
$0g_{\frac{7}{2}}$	0.99175	0.12822	5.37529
$0g_{\frac{9}{2}}$	0.41651	0.90913	1.43738
$2p_{\frac{1}{2}}$	0.99989	0.01482	15.29215
$2p_{\frac{3}{2}}$	0.99986	0.01650	14.09936
$1f_{\frac{5}{2}}$	0.99986	0.01648	16.10043
$1f_{\frac{7}{2}}$	0.99983	0.01848	12.32801
$0h_{\frac{9}{2}}$	0.99937	0.03541	15.32542
$0h_{\frac{11}{2}}$	0.99818	0.06026	6.89595

The pairing strength values for Sn-114 were determined to be $G_N = 0.96215$ and $G_P = 1.00000$, with the proton case left as default due to Sn-114 being magic proton-wise. This leads to discrete proton levels as can be seen in the occupation amplitude numbers.

Table 35: Neutron state quantum numbers, occupation amplitudes and quasi-particle energies for Sn-114

State	u	v	E_{qp}
$1p_{\frac{1}{2}}$	0.08983	0.99596	8.33508
$1p_{\frac{3}{2}}$	0.08065	0.99674	9.65648
$0f_{\frac{5}{2}}$	0.06889	0.99762	10.18446
$0f_{\frac{7}{2}}$	0.05753	0.99834	13.54673
$2s_{\frac{1}{2}}$	0.79612	0.60513	1.32733
$1d_{\frac{3}{2}}$	0.88439	0.46675	1.52432
$1d_{\frac{5}{2}}$	0.34535	0.93847	2.04209
$0g_{\frac{7}{2}}$	0.47281	0.88116	1.57340
$0g_{\frac{9}{2}}$	0.11533	0.99333	6.21154
$2p_{\frac{1}{2}}$	0.99941	0.03448	8.19936
$2p_{\frac{3}{2}}$	0.99920	0.04011	7.36802
$1f_{\frac{5}{2}}$	0.99901	0.04447	9.16586
$1f_{\frac{7}{2}}$	0.99748	0.07095	6.15930
$0h_{\frac{9}{2}}$	0.99795	0.06393	8.94017
$0h_{\frac{11}{2}}$	0.95619	0.29276	2.12733

Table 36: Proton state quantum numbers, occupation amplitudes and quasi-particle energies for Sn-114

State	u	v	E_{qp}
$1p_{\frac{1}{2}}$	0.00576	0.99998	3.78740
$1p_{\frac{3}{2}}$	0.00397	0.99999	5.35632
$0f_{\frac{5}{2}}$	0.00364	0.99999	6.12138
$0f_{\frac{7}{2}}$	0.00213	1.00000	10.09915
$2s_{\frac{1}{2}}$	1.00000	0.00247	4.83083
$1d_{\frac{3}{2}}$	1.00000	0.00303	5.33967
$1d_{\frac{5}{2}}$	0.99998	0.00590	2.53197
$0g_{\frac{7}{2}}$	0.99998	0.00625	3.20727
$0g_{\frac{9}{2}}$	0.00662	0.99998	2.85522
$2p_{\frac{1}{2}}$	1.00000	0.00060	12.93079
$2p_{\frac{3}{2}}$	1.00000	0.00069	11.68079
$1f_{\frac{5}{2}}$	1.00000	0.00069	13.73080
$1f_{\frac{7}{2}}$	1.00000	0.00091	10.13216
$0h_{\frac{9}{2}}$	1.00000	0.00124	13.16315
$0h_{\frac{11}{2}}$	1.00000	0.00309	4.85415